ADDIS ABABA UNIVERSITY
ADDIS ABABA INSTITUTE OF TECHNOLOGY
SCHOOL OF MECHANICAL AND INDUSTRIAL ENGINEERING

ANALYSIS OF MECHANICAL AND THERMAL LOADS EFFECTS ON WHEEL-RAIL MATERIAL DURING SLIPPAGE

BY
ABDULHAKIM MERDASSA

MARCH 2015
ADDIS ABABA, ETHIOPIA

ADDIS ABABA UNIVERSITY

ADDIS ABABA INSTITUTE OF TECHNOLOGY

SCHOOL OF MECHANICAL AND INDUSTRIAL ENGINEERING

Analysis of mechanical and thermal loads effects on Wheel-rail material during slippage

A Thesis submitted to the School of Graduate Studies of Addis Ababa Institute of Technology in Partial Fulfillment of the Requirement for the Degree of Masters of Science in Mechanical Engineering (Railway Engineering)

By

ABDULHAKIM MERDASSA

ADVISOR

HABTAMU TKUBET

March, 2015

ADDIS ABABA

ADDIS ABABA UNIVERSITY

ADDIS ABABA INSTITUTE OF TECHNOLOGY SCHOOL OF

MECHANICAL AND INDUSTRIAL ENGINEERING

Analysis of mechanical and thermal loads effects on Wheel-rail material during slippage

By

Abdulhakim Merdassa

March, 2015

Approved by Board of Examining:

Birhanu Beshah (Dr.)	Birhanu Beshah(PhD) Head,Railway Engineering Centre	21/05/15
Head, railway center	Signature	Date
Ato Habtamu Tkubet (MSc.)		21/05/15
Advisor	Signature	Date
Ato Tollosa Dreibsa (MSc)		18/05/2015
Internal Examiner	Signature	Date
Daniel Tilahun (Dr.)		21/05/15
External Examiner	Signature	Date

Director of Postgraduate Program
Addis Ababa University
Addis Ababa Institute of Technology

ADDIS ABABA UNIVERSITY

ADDIS ABABA INSTITUTE OF TECHNOLOGY

CHOOL OF MECHANICAL AND INDUSTRIAL ENGINEERING

DECLARATION

he undersigned, declare that this thesis is my original work and has not been presented for degree in any university and all the sources of materials used for the thesis have been y acknowledged.

bdulhakim Merdassa		18/05/2015
Name	Signature	Date

ADDIS ABABA UNIVERSITY

ADDIS ABABA INSTITUTE OF TECHNOLOGY SCHOOL OF

MECHANICAL AND INDUSTRIAL ENGINEERING

Analysis of mechanical and thermal loads effects on Wheel-rail material during slippage

By

Abdulhakim Merdassa

March, 2015

Approved by Board of Examining:

Birhanu Beshah (Dr.)	____________________	____________________
Head, railway center	Signature	Date
Ato Habtamu Tkubet (MSc.)	____________________	____________________
Advisor	Signature	Date
Ato Tollosa Dreibsa (MSc)	____________________	____________________
Internal Examiner	Signature	Date
Daniel Tilahun (Dr.)	____________________	____________________
External Examiner	Signature	Date

Acknowledgement

Firstly, I would like to express my deepest gratitude to my advisor Ato HABTAMU TKUBET, for his constant motivation, guidance, support, supervision and constructive suggestion throughout this thesis work.

In addition gratefully acknowledge the Ethiopian railway corporation institute and Ethiopian railway cooperation for financial support through providing me the scholarship opportunity and sponsoring for Graduate studies.

Finally, I would like to thank my entire friends for encouraging me through these many years of school. They have all been a tremendous source of support and encouragement throughout all of this work. I appreciate their interest in my paper.

Abstract

Slippage is the main cause of damage and strength reduction of rail/wheel material. During rail-wheel rolling contact there always exist micro slippages at contact area. Even if normal movement of railway wheel is combination slip-stick phenomena, slippage will cause severe effect the wheel and rail material. This paper focus on the analysis of effects of longitudinal slippages at rail head and wheel tread contact area based on elastic-plastic model by introducing elastic and plastic material model for the rail and wheel. The normal load is analyzed with both hertz and FE method whereas the tangential load is analyzed using Coulomb's and Johnson/vermulen method. Beside, Surface temperature of the interface for different slip velocity is estimated analytically. The loads and boundary condition are simulated for over contact area in order to predicate the effect using ANSYS 15 commercial software. Based on the analysis and simulation the loads that developed during longitudinal slippage create the high thermo-mechanical stress on contact area. This cause plastic strain development and reduction of stress fatigue life for the increased value of loads that resulted from slippage as can note from analysis and simulation results.

Table of contents

Acknowledgement--ii

Abstract--iii

Table of content ---iv

List of figures ---vii

List of table --ix

Nomenclatures--x

CHAPTER ONE: INTRODUCTION --1

1.1 Background of the problem---1

1.2 Significant of the study ---2

1.3 Problem statement ---3

1.4 Objective of the study--4

1.4.1 General objective---4

1.4.2 Specific objective---4

1.5 Research methods---5

1.5.1 Data collection--5

1.5.2 Data analysis--5

1.5.3 Presentation of the Research--6

1.6 Scope of the study--7

1.7 Limitation of the study--7

CHAPTER TWO: LITERATURE REVIEW --8

2.1 LITERATURE REVIEW---8

CHAPTER THREE: THEORETICAL BACKGROUND---------------------------10

3.1 Rail-wheel contact slippage---10

3.2 Adhesion force and adhesion coefficient--------------------------------11

3.3 Relation of adhesion coefficient and slip velocity---------------------12

3.4 Automatic anti-slip controls--13

3.5 Mechanical and thermal loads at rail-wheel contact area-------------13

3.5.1 Mechanical Loads--13

3.5.2 Thermal Loads---14

CHAPTER FOUR: MODELING --15

4.1 Geometrical Model of physical problem-------------------------------15

4.2 Contact modeling--17

4.3 Yield criteria---17

4.4 Work hardening model approach--18

4.5 Stress life analysis approach --19

CHAPTER FIVE: ANALYSES --21

5.1 Mechanical load analysis --21

5.1.1 Contact pressure analysis --------------------------------------21

5.1.2 Tangential load analysis--24

5.1.3 Contact stress-stain analysis due to mechanical loads ------25

5.1.3.1 FEM solution steps for mechanical analysis---------25

5.2 Thermal load analysis--28

5.2.1 Heat flux analysis at contact area ----------------------------28

5.2.2 Temperature rise analysis at contact area---------------------31

5.2.3 Comparison with Heat flux and contact temperature during barking---33

5.2.4 Contact Stress-stain analysis due to thermal load -----------33

5.2.4.1 FEM solution steps for thermal analysis --------33

5.3 Simulation of combined thermo-mechanical loads effect at contact area--34

5.3.1 Temperature dependent property of the materials --------34

5.3.2 Boundary condition for combined load simulation---------35

CHAPTER SIX: RESULTS AND DISCUSSION ---------------------------------37

6.1 Results---37

6.1.1 Mechanical load stress-strain analysis result ------------------37

6.1.2 Thermal stress analysis result-----------------------------------39

6.1.3 Combined thermo-mechanical load effect analysis results----42

6.2 Discussion---54

CHAPTER SEVEN: CONCLUSION AND RECOMMENDATION ---------------57

7.1 Conclusion ---57

7.2 Recommendations---58

7.2 Future works --59

References --60

Annex: Important tables ---62

List of Figures

Figure 1: Adhesion-slip velocity characteristic shape------------------------------12

Figure 2: Forces and velocities that act on wheel----------------------------------14

Figure 3: UIC-60 Rail and wheel profiles models---------------------------------15

Figure 4: Rail-wheel assembly modes on CATIA rail head to wheel tread contact--16

Figure 5: Contact element command Tree---17

Figure 6: Isotropic hardening with change in yield surface------------------------18

Figure.7: Kinematic hardening with translation of yield surface center axis----18

Figure 8: The Stress-Life (S-N) Curve draw to logarithmic plot------------------19

Figure 9: Wheel/rail configuration showing different principal relative radii of curvature---21

Figure 10: Mesh of rail-wheel assembly---26

Figure 11: Rail and wheel Contact pair--27

Figure 12: Boundary condition for stress-strain analysis due to mechanical load--27

Figure 13: Elliptical area of the contact---29

Figure14: Coordinate systems for temperature calculation in wheel/rail contact respectively---29

Figure 15: Ansys workbench setting for combined load case analysis-----------35

Figure 16: Mechanical load setting at imported thermal load for combined analysis---36

Figure 17: Stress at contact area due to mechanical load-------------------------37

Figure 18: Elastic strain at contact area due to mechanical load------------------38

Figure 19: Contact area stress life during mechanical load only------------------38

Figure 20: Contact area thermal stress for 2.33 m/s slip velocity simulation----40

Figure 21: Contact area thermal stress for 4.55 m/s slip velocity simulation----40

Figure 22: Contact area thermal stress for 6.77 m/s slip velocity simulation----41

Figure 23: Contact area thermal stress for 8.99 slip velocity simulation---------41

Figure 24: Equivalent von mises stress at 2.33 m/s slip velocity simulation----43

Figure 25: Equivalent von mises stress at 4.55 m/s slip velocity simulation----43

Figure 26: Equivalent von mises stress at 6.77 m/s slip velocity simulation----44

Figure 27: Equivalent von mises stress at 8.99 m/ slip velocity simulation-----44

Figure 28: Elastic strain over contact area at 2.33 m/s slip velocity-------------45

Figure 29: Elastic strain over contact area at 4.55 m/s slip velocity-------------45

Figure 30: Elastic strains over contact area at 6.77 m/s slip velocity------------46

Figure 31: Elastic strains over contact area at 8.99 m/s slip velocity------------46

Figure 32: Thermal strain over contact area at 2.33 m/s slips velocity-----------48

Figure 33: Thermal strain over contact area at 4.55 m/s slips velocity-----------48

Figure 34: Thermal strain over contact area at 6.77 m/s slips velocity-----------49

Figure 35: Thermal strain over contact area at 8.99 m/s slips velocity-----------49

Figure 36: Plastic strain distribution over contact area at 2.33 m/s and 4.55 m/s slips velocity ---50

Figure 37: Plastic strain distribution over contact area at 6.77 m/s and 8.99 m/s slips velocity--50

Figure 38: Equation and graphical representation of the Gerber Mean Stress correction for Stress Life Fatigue Analysis--------------------------51

Figure 39: Stress life at contact area for 2.33 m/s slip velocity simulation------52

Figure 40: Stress life at contact area for 4.55 m/s slip velocity simulation------52

Figure 41: Stress life at contact area for 6.77 m/s slip velocity simulation------53

Figure 42: Stress life at contact area for 8.99 m/s slip velocity simulation------53

List of Tables

Table 1: Temperature dependent property of the materials used for the analysis--34

Table 2: Result summary of heat flux and max temperature at rail surface------39

Table 3: Result summary of heat flux and max temperature at wheel surface---39

Table 4: Summary of loading condition for combined thermal and mechanical simulation---42

Table 5: Comparison of maximum equivalent thermal stress and combined stress at different slip velocity---54

Table 6: Comparison of maximum thermal strains at different slip velocity-----55

Table 7: The of value of maximum elastic and plastic strain from combined loads--- 55

Table 8: Comparison of minimum strain life during combined loads condition---56

Table 9: Hertz coefficient m and n quantities--------------------------------------62

Table 10: Kalker coefficient table from reference --------------------------------62

Table 11: Adding of thermal (a) mechanical (b) material property data for combined load analysis at 100 ^{o}C surface temperature-------------63

Nomenclatures

a - Major semi-axis (ellipse) of contact patch

b - Minor semi-axis of contact patch ellipse

$K1$ - Constants that depend on the material properties of wheel

$K2$ - Constants that depend on the material properties of rail

$R22$ -The principal transverse radius of curvature of the wheel

$R21$-The principal transverse radius of curvature of the rail

$\tau._x$ - Normalized creepage value in longitudinal direction

ε - Heat partitioning coefficient between rail and wheel

$\phi._r$ - Heat flux in to rail at the contact area of rail and wheel

$\phi._w$ - Heat flux in to wheel at the contact area of rail and wheel

V - Vehicle forward speed in longitudinal direction

$\Theta._r$ - Rail surface temperature rise at contact area

$\Theta._w$ - Wheel surface temperature rise at contact area

$R11$ - The principal rolling radius of the wheel

$R22$ - The principal rolling radius of the rail

UIC - International union of railways

Po - maximum Contact pressure

ω - Angular velocity of wheel

m & n - Hertz coefficients

C_{11} - Kalker contact coefficient

ξ – Longitudinal of creepage

CHAPTER ONE

INTRODUCTION

1.1 Background of the problem

Wheel sipping is a serious problem in railways vehicles. It results extensive damage to wheel and rail material. As it is known the greatest effort is required from a locomotive when starting. At this time, if the driver applies too much power to the wheels, the turning force applied to the wheel will greatly exceed the opposing friction force and the wheel will turn without being able to move the train forward. If the driver does not take quick corrective action the locomotive can end up stationary with its wheels spinning. This can damage the rail-wheel surface, which, in extreme cases, can cause rail surface burn. High-speed passenger trains usually under take high accelerations or decelerations near stations which require high adhesion coefficients to control slippage.

When the traction forces exceed the available adhesion, gross slipping occurs which generates heat at the wheel-rail contact zone. The consequent rise in temperature probably increases wheel and rail wear, and low cyclic fatigue. In the extreme case of slipping, the temperatures generated may be high enough to cause metallurgical transformation of the wheel or rail material.

Some locomotive types were more prone to this phenomenon than others. Especially the effect is much more likely to occur with a heavier train and faster trains where the rail surface is compromised, for example, during wet or icy weather, or when there is oil or leaves on the track. Wheel can slip on the rail at longitudinal direction on rail head and lateral direction at gauge side of rail specially at curving. When we consider longitudinal slippage, micro and partial and sometimes full slippage can occur on rail head and wheel tread contact during traction.

The continuing improvements in traction performance of railway vehicles demand the optimum use of the available wheel-rail adhesion. Modern locomotives are more powerful and reach higher speeds. A few milliseconds of time the slip between wheel and rail becomes large can cause small material volumes in the contact to be heated several hundred degrees Celsius temperature. Calculation of the maximum temperature is an important part in the investigation of thermal load. The thermal stresses have to be superimposed on the mechanical contact stress in order to see the overall impact on rail and wheel assembly.

Many research results have confirmed the dominant influence of thermal loads in regard to mechanical loads during slippage. Although a number of studies have been focused on the influence of slip on rail wheel contact, very limited information regarding the contact stress, thermal load and effect on material during traction is available. Since the contact temperature and stress can hardly measure during slippage, numerical modeling and analysis becomes an important measure in the investigation of wheel-rail contact problems.

Therefore it is important assess the causes of the wheel/rail slipping, stress generation at contact region and the overall effect impose on rail wheel material for life time prediction ,maintenance and risk minimization of railway operation.

1.2 Significant of the study

The contacts temperatures under real railway operating conditions can hardly are measured. Thermal damage on wheels and rail is great problem in during slippage, as it can lead to thermal stress, reduction of service life and deterioration of profiles. In addition structural load analysis is involved in almost every kind of physical processes and it can be the limiting factor for many processes.

Slipping has always been major problems in the railway Industry, due to the low friction between rail and wheel. Many researchers have tried to assess influence of mechanical loads and thermal load induced by sliding contact. It is important to determine with high precision the pressure and temperature field of the wheel/rail contact area.
Furthermore, modeling of thermo-mechanical effects has become increasingly important in product design railway (e. g. wheel and rail rolling contact, traction braking systems, and so on).

1.3 Problem statement

Slip between wheel and rail is common phenomena in train operation even if the extent varies. The most significant one is loss of adhesion during tractive effort this cause significant heat generation at the contact between rail and wheels. The result is high wear of rail/wheel material. In order to predict these phenomena an accurate understanding of the thermal and mechanical loads the contact is required. Since it is difficult to measure the maximum temperature and pressure on wheel-rail contact area during slippage it important to approximate and analyze using analytical and FEM. In this paper this type of problem is being discussed. In the first the response of rail and wheel due to thermal and mechanical loading are dealt and in the second the combined loading is being analyzed. This research is proposed to address at least following questions:-

- How slippage arises at wheel and rail contact during operation?
- What will be the pressure and temperature distribution and the maximum temperature in wheel/rail contact?
- What will be thermal and mechanical stress induced in rail and wheel material during slippage?
- What will be significant effect of wheel slip on rail/wheel material?

Such and other kinds of questions divert the interest of most researchers to direct their attentions to study stress on rail-wheel contact area in order to reduce defect and proper selection of their design materials.

1.4 Objective of the study

1.4.1 General objective

The main aim of this study is to model and analyze the thermo-mechanical load between wheel and rail during slippage using semi-analytical and finite element method and their impact on the wheel and rail material.

1.4.2 Specific objective

- Analysis of mechanical load acting at rail and wheel contact area
- Analysis of thermal loads acting at rail and wheel contact area
- Modeling and analysis of combined thermal and mechanical loads
- Stress-strain analysis at contact area by using temperature dependent thermal and mechanical property of rail/wheel material
- Predicted the effects of theses load on of rail and wheel material
- By means of software simulation visualize and interpreting of the slippage effect on contact area of rail and wheel

1.5 Research methods

The methodology that has been chosen in order to acquire information, make analysis and deduce conclusions about the subject matter is based on the following measures;

1.5.1 Data collection

For the purpose of this research, and in order to achieve the objectives listed in the sub topic of specific objective of the research the data is collected through secondary data collection method:

- By browsing different published papers and journals
- By browsing different thermo-mechanical analysis related books in rail-wheel contact
- By Reading other recent related research works that have been done before by other researchers.
- By visiting to the Ethiopian rail way cooperation, in order to get specification of existing railway facility.

1.5.2 Data analysis

In this sub topic the overall procedure of data analysis is stated as clear as possible as in the following manner sequentially having in minds that specific question to answer.

- State clearly basic principle behind wheel-rail slip phenomena based on gathered data and references.
- 3D Modeling of physical problem is done by CATIA commercial software
- Based on analytical models, the normal load is calculated by hertizian method and FEM whereas tangential load is analyzed by Johnson /vermulen method
- Heat flux and contact temperature during gross slip is calculated analytically.

- The geometric model and the contact load estimated during slippage are transfer to FEM analysis software/ ANSYS and simulated effects of slippage on rail wheel material.

1.5.3 Presentation of the Research

- Pictorial as well as tabulated presentation of findings and state their scientific meaning by using different software
- Analyze and interpret the findings. Discuss each finding and relate with specific research objectives
- Writing conclusion and recommendations or future development (if any) to investigate further more by other researchers later on.
- Acknowledge for the materials used to prepare the research or for any one who helps to facilitate your work.
- Finally editing the overall paper to submit and preparation of presentation materials.

1.6 Scope of the study

A railway car axel load of 25KN used for this study which is the load applied on single wheel will be 12.5KN. UIC standard is applied to model the rail and wheel profile geometry. The material used for this analysis and simulation is carbon steel having identical material property for both. The 3D-quasi-static numerical and semi analytical analysis is carried out for longitudinal slippage effect. The analytical analysis and simulation is carried out for straight track and constant friction coefficient condition in order to see the effect of slippage on rail and wheel material around the contact region.

1.7 Limitation of the study

Experimental testing and simulation of thermo-mechanical effect on wheel/rail material during slippage was helpful to compare the semi-analytic FE result but due to lack full laboratories the study does not include experimental test and simulation. The effect of slippage is analyzed indirectly by analytical estimation of contact loads and temperature; the result will be more accurate if the real time effect modeling and simulation software is employed. Because of lack tested monotonic and cyclic strength material properties of rail and wheel, strain life and hysteresis analysis cannot be performed.

CHAPTER TWO

LITERATURE REVIEW

2.1 Literature review

Slippage is great problem for locomotive which do not have slip control. In order to address the problem research have tried to model and analysis its effect starting early times. Some of them are discussed as follow. Temperature rise due to slip between wheel and rail-an analytical solution for hertzian contact presented in 1980[1]. The analysis of temperature rise is performed by the Laplace transform method by making the approximations that the heat flow is linear into a semi-infinite solid and the moving heat source is treated as quasi-static.

A band source of heat moving along the surface of a semi-infinite solid considered, i.e. $z > 0$, at a uniform speed. The assumption made is that the heat source is of infinite width perpendicular to the direction of motion and of length 2a in the direction of motion. It supplies heat uniformly along its width while the heat distribution along its length is elliptical. Mathematical relation of heat flux and temperatures between rail-wheel gross slip is presented in his work. After passing through the contact area as the element of area leaves the contact zone the heat input becomes zero and the surface temperature decays by conduction into the bulk material.

Thermo-elastic–plastic finite element analysis of wheel/rail sliding contact previously performed [2]. A finite element method (FEM) is used to study thermal-elastic–plastic deformation and residual stress after wheel sliding on a rail. The consideration of sliding contact between the wheel and rail is restricted to a two dimensional contact problem. The repeated sliding contact process is simulated by translating the normal contact pressure and the tangential traction across the rail surface. The normal contact pressure is idealized as the hertzian distribution, and tangential force is modeled by Coulomb model. The heat-convection and radiation between the rail and ambient, the material mechanical and thermal coefficients changing with temperature are taken into account.

Based on their loading condition, during mechanical load without thermal load analysis no plastic strain is notice on contact, but during thermal and mechanical load case it increased by 0.36 %. The maximum noticed thermal and residual stress is 408Mpa and surface temperature is 637^{o}C for wagon. Generally the wheel/rail friction thermal load has a significant influence on deformation, residual stress and plastic strain at the rail surface.

Rail life prediction for tramcars under full slip regime is examined earlier [3]. The influence of the rail material strength, in terms of its yield shear stress, is also analyzed. In order to determine the accumulation of strain for the simulated maneuvers, a (local) 3D grid below each contact area is considered. At each node of this grid the stress tensor is calculated using Boussinesq-Cerruti equations (elastic half-spaces) the accumulation of strain is estimated, the results presented in this paper are referred to a fully loaded tramcar vehicle running on a 50 m radius curve, 15km/h, and with low level of rail irregularity. The value of k_{eff} (effective shear yield Stress) strongly affects the damage and strain accumulation and rail life. In this particular study, both side of rail wheel contact simulated .i.e. left and right wheel rail assembly are simulated using computer program in order to see the damage from the loading condition.

In my paper, I have tried to focus on elastic-plastic thermal and mechanical contact stress and strain analysis that caused by slippage based on quasi-static load consideration using ANSYS V15 commercial software. Mechanical loads and heat flux /temperature will be applied over contact area for specific duration time is simulated in order to see the effect on the materials. The result of stress and strain is compared and analyzed in order to predicate the strain amount and stress life at rail-wheel contact area.

CHAPTER THREE
THEORETICAL BACKGROUND

3.1 Rail-wheel contact slippage

One of the most common problems in railway industry is rail-wheel contact slippage. Based on the slip theory during slippage driven wheel does not roll, but actually rotates faster/slower than the corresponding longitudinal velocity of the vehicle. The difference between the angular velocity of the wheel and the corresponding longitudinal velocity causes the slip. [4]

The slippage can be defined for every wheel as follow;

$$S = \frac{\text{V rel}}{\text{Vmean}} = \frac{\omega.r - v}{0.5(\omega.r + v)} \tag{1}$$

Where ω angular velocity of wheel, V vehicle forward speed r is is the radius of the wheel. and the Slip ratio is defined by;

$$\text{Slip} = \frac{\text{Vehicle speed} - \text{Wheel speed}}{\text{Vehicle speed}} \tag{2}$$

Sometimes a separate definition of the slip is used when the slip velocity is negative and positive. In railway vehicles the traction procedure is slightly different. During traction it is taken to be negative whereas during braking it is taken to be positive.

3.2 Adhesion force and adhesion coefficient

The Definition of the adhesive force is the force of attachment between two contacting objects. If this definition is translated in to a railway definition, it will be the ability of the wheel to exert the maximum traction force on the rail and still maintain persistence of contact without exceeding the optimal slip. Thus adhesion is the amount of force available between the rail and the wheel. Therefore, one can say that the adhesive force comes about as a result of the frictional forces [4]. The adhesive force is given by:

$$F_a = \mu_a \, F_N = \mu a \; ma \; g \tag{3}$$

Where Fa is the adhesive force, μ_a is adhesion coefficient, F_N is the normal force, ma is the adhesive mass of the vehicle and g is the gravitational constant. The adhesive mass is defined by the total mass on all the driven wheels. The adhesive force Fa changes in time, though the normal force F_N is constant, which implies that the adhesion coefficient μa changes in time. The adhesion coefficient (μ_a) is limited by the friction coefficient (μ_f). As it is known friction coefficient is the ratio of friction force and normal load whereas adhesion coefficient is the ratio of tractive force and normal load.

This is analogous to the case of a wheel rolling along a rail. The wheel is subject to normal force, F_N and travels along the rail at velocity v. The wheel is subject to torque T, which maintains the angular velocity of the wheel, ω, and also causes a reactive tangential force, F_T at the wheel–rail interface. The tangential force of a driving wheel is known as traction, which ultimately propels the wheel along the rail. During deceleration, the tangential force, F_T opposes the running direction due to the braking torque, T applied anticlockwise. The tangential force in the longitudinal direction during both acceleration and deceleration is referred to as adhesion. The ratio between the adhesion force and the normal force is known as the adhesion coefficient [4].

$$\mu a = \left(\frac{Fa}{F_N}\right) \leq \mu f \tag{4}$$

3.3 Relation of adhesion coefficient and slip velocity

The force that is transmitted between wheels and rail is called the tangential force. The tangential force is transmitted by a small contact area between the wheel and rail having area of a few square centimeters. The maximum value of the tangential force depends on the adhesion coefficient and the locomotive adhesion weight. As mentioned earlier both parameters vary in time and locomotive position on the track. The adhesion coefficient in turn depends on the slip velocity, conditions of rail surface, a train velocity and temperature in the contact area.

An adhesion-slip characteristic which shows the dependence of the adhesion coefficient on the slip velocity or slip is shown in Fig.2 bellow which is simulated for slip velocity against adhesion coefficient [4]. Based on the simulation graph the characteristic curve is divided into three areas. The first area is called a linear area. In this area the adhesion coefficient depends approximately linearly on the slip velocity. The second area is called nonlinear area. Both areas are called as a stable area of the adhesion-slip characteristic. The third area is called the unstable area. The slip velocity affects value of the adhesion coefficient from zero to its maximum value.

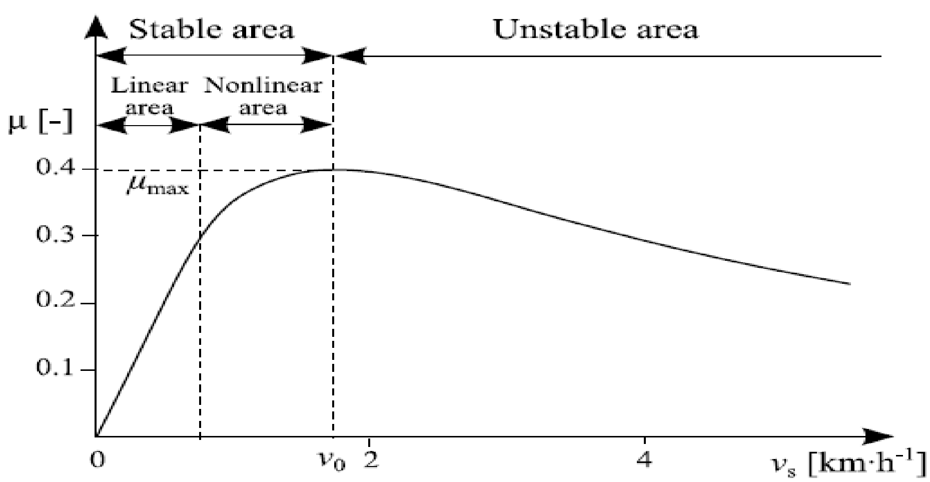

Figure 1: Adhesion-slip velocity characteristic shape [4]

The longitudinal speed of vehicle also has effect on adhesion coefficient. The maximum value of the adhesion coefficient decreases when the longitudinal velocity increases. The dependence according Curtius and Kniffler [4] can be expressed as

$$\mu\ \max = \frac{7.5}{V_L + 44} + 0.161 \qquad (5)$$

Where V_L longitudinal velocity and μ max is maximum adhesion coefficient.

3.4 Automatic anti-slip controls

Total locomotive tractive effort of a railway car depends on the sum of individual tangential forces that are transmitted by every wheel. The maximum value of the tractive effort can be achieved when a slip velocity of every driven wheelset is controlled to an appropriate value. The slip controller beside of improving tractive effort minimizes damages and losses on rail car e.g. through decrease wear of the wheels and rails or by avoid mechanical damage of the locomotive. In order to decrease the effects of slippage on rail-wheel material slip controls play great role. Slippage can cause burning of rail surface if not correct quickly. Quicker response is obtained through automated control method like Anti slip controllers. The methods use a broad knowledge of electrical engineering, control technology and mechanical engineering. [4]

3.5 Mechanical and thermal loads at rail-wheel contact area

3.5.1 Mechanical Loads

Rolling/slip contact loads in rail-wheel contact region create the greatest mechanical stress fields. Axle load is transferred into wheels and crate high stress on contact. Other mechanical loads, such as friction force between rail and wheel affect mechanical stress fields of the wheel. In many previous works, the effects of these forces were ignored. But here, for having the reliable model, it better to use 3D FEM for modeling rail-wheel contact with hertzian and FEM analysis approach in order obtain the most accurate responses [5].

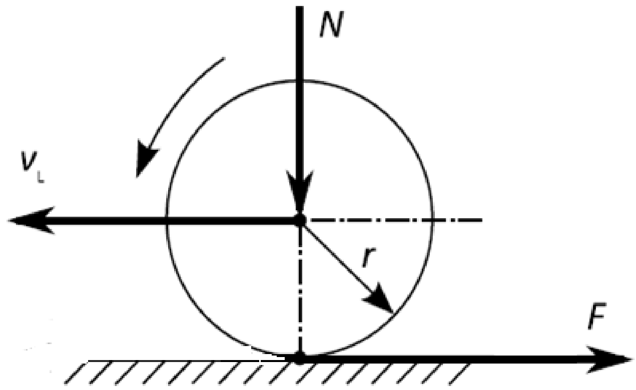

Figure 2: Forces and velocities that act on wheel

3.5.2 Thermal Loads

The main source of heat generation at the contact area between rail and wheel is friction force. The slip between wheel and rail causes frictional heating of both bodies. The maximum surface temperature during rolling contact of railway wheels with sliding friction can be estimated using Blok's flash temperature formula as presented in section 5.2.2. In this case not only the convection at the free wheel surfaces but also the heat conduction from the wheel into the colder rail has to be considered. In addition for determining temperature rise of these components, it is necessary to know the heat partition factor of rail and wheel contact regions. At the beginning of wheel sliding on the rail, heat partition factor between rail and wheel is equal to 0.5. This is due to considering the same physical and thermal properties for the wheel and rail. By increasing the slip time, this factor reduces, which means that the most of heat generated due to slip is transferred to rail. The reason for this reduction can be based on the fact that during rotation of the wheel on the rail, a new rail surface is always subjected to the high temperature wheel surface. [5]

CHAPTER FOUR

MODELING

4.1 Geometrical model of physical problem

For modeling the wheel and rail, profile of railway car is used which have wheel diameter of 840 mm which is amongst the most common wheels in the world fleet was applied. UIC60-rail is modeled with S1002 wheel and the sample length of 600 mm considered. In this study an axle load of 25,000N which is 12 500 N loads on a wheel of passenger car running 33.4 m/s on the straight track is considered.

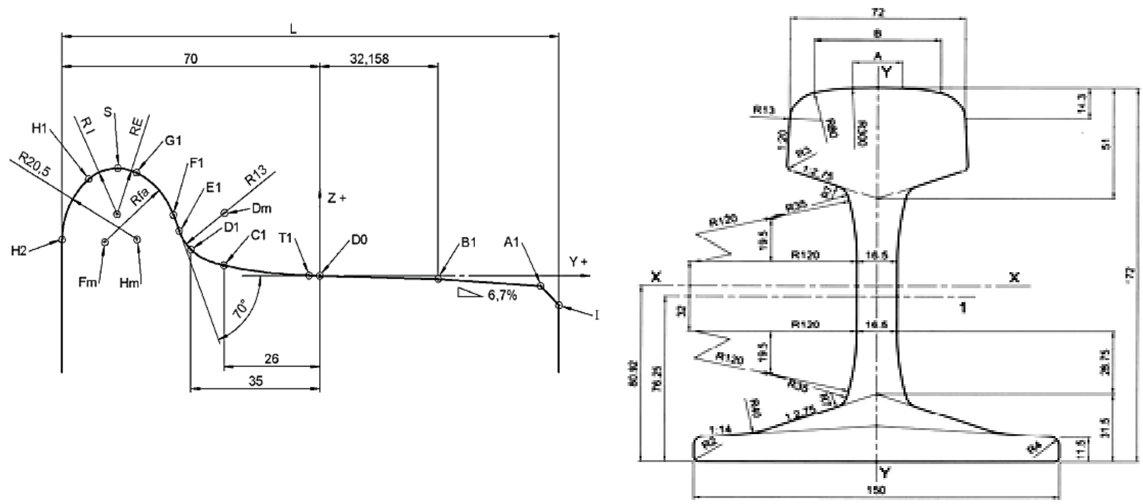

Figure 3: UIC-60 Rail and wheel profiles models [6], [7]

The 3D model of the 840 mm diameter wheel and 600 mm long rail is model using CATIA R19 V5 for simulation of rail head and wheel tread contact.

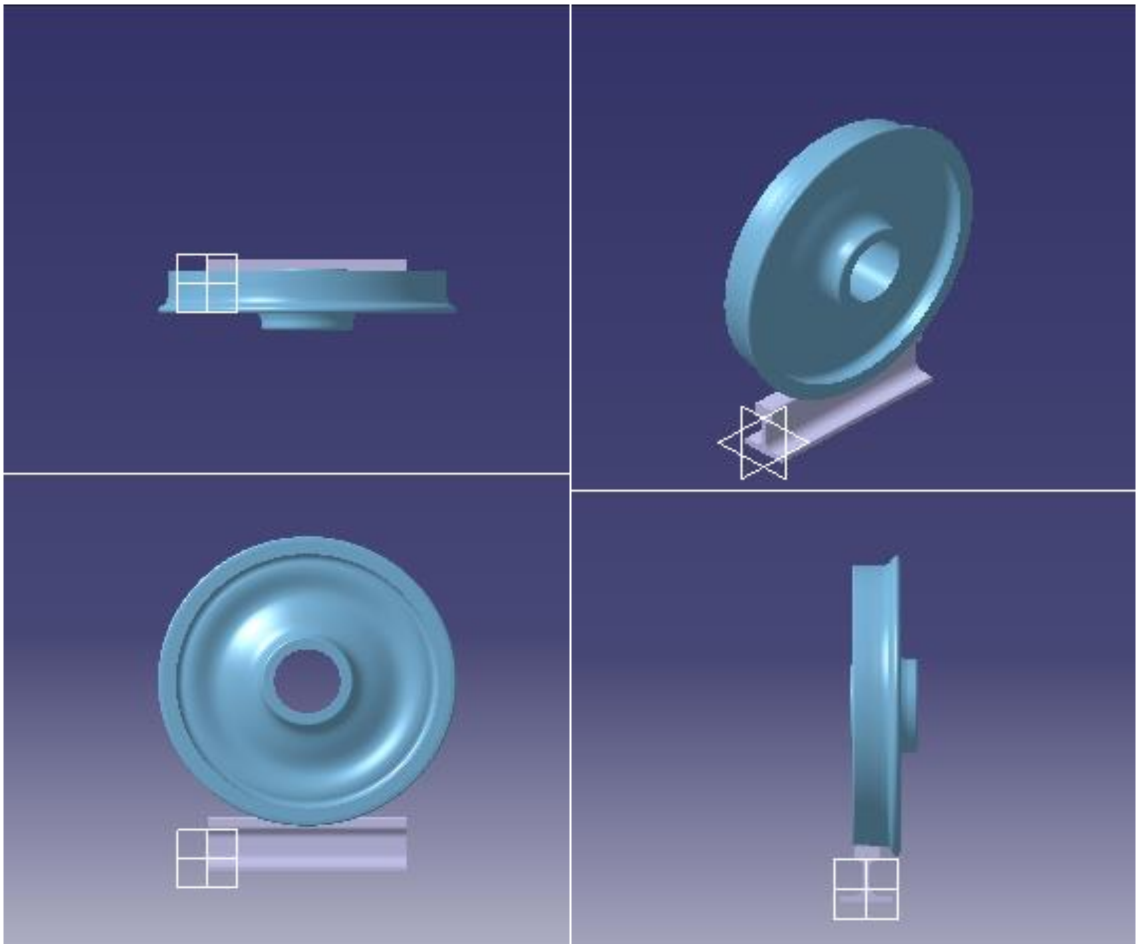

Figure 4: Rail-wheel assembly modes on CATIA rail head to wheel tread contact

4.2 Contact modeling

Contact zone with surface temperature is created by means of sub modeling on wheel as well as on rail contact point in ANSYS. The contact stiffness is selected to be augmented Lagrange contact stiffness of solid to solid surface contact method. It is recommended for general frictionless or frictional contact in large-deformation problems. Augmented Lagrangian method is very similar to that of penalty method except that it reduces sensitivity to contact stiffness. Beside the contact is modeled to have Symmetric behavior. This means that the Contact surfaces are constrained from penetrating the Target surfaces and the Target surfaces are constrained from penetrating the Contact surfaces are. The element type for contact area is Contact 174 and for target area is Target 170.

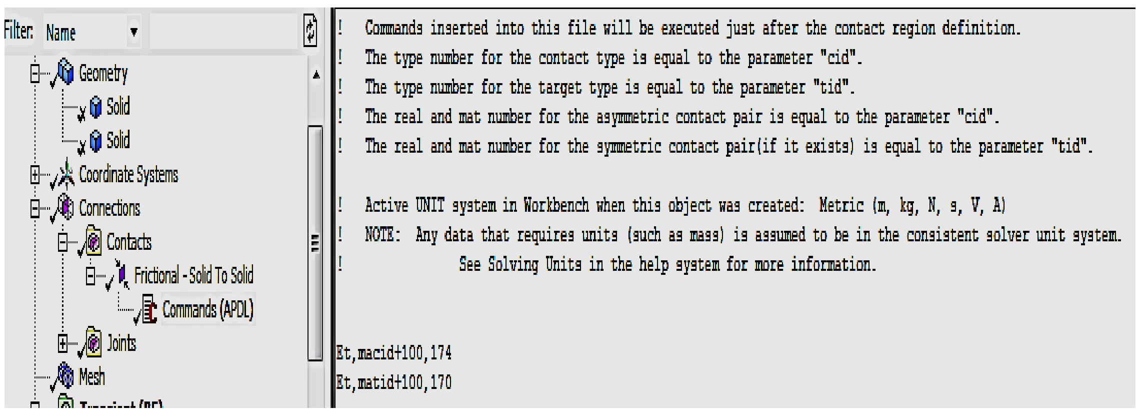

Figure 5: Contact element command Tree

4.3 Yield criteria

The yield criterion determines the stress level at which yielding of a material will occur. The yield criteria can be expressed in terms of the stress state, strain state, and strain energy quantity. The common yield, known as the von Mises yield criterion predicts that yielding will occur whenever the distortion energy in a unit volume equals the distortion energy in the same volume when uniaxial stressed to the yield strength.

From this theory, a scalar invariant (Von Mises equivalent stress) is derived as [8].

$$\sigma_e = \sqrt{\left(\frac{1}{2}\right)[(\sigma_1 - \sigma_2)^2 + (\sigma_{2-}\sigma_3)^2 + (\sigma_3 - \sigma_1)^2]} \tag{6}$$

When von Mises equivalent stress exceeds the uniaxial material yield strength, general yielding will occur.in this study von mises stress yield criteria is implement for stress analysis.

4.4 Work hardening model approach

The importance of nonlinear material behavior effects numerous practical applications. While the assumption of linear behavior leads to a reasonable idealization of structural behavior, there are situations where nonlinear effects must be incorporated for a more realistic assessment of the structural response. Hardening rules describes how the yield surface changes (size, center, and shape) as the result of plastic deformation. There are two hardening rules isotropic and kinematic hardening rules. Isotropic hardening is where the yield surface size changes, but the center axis and the general shape of the yield surface do not change. Kinematic hardening is that the yield surface remains constant in size and translates in the direction of yield.

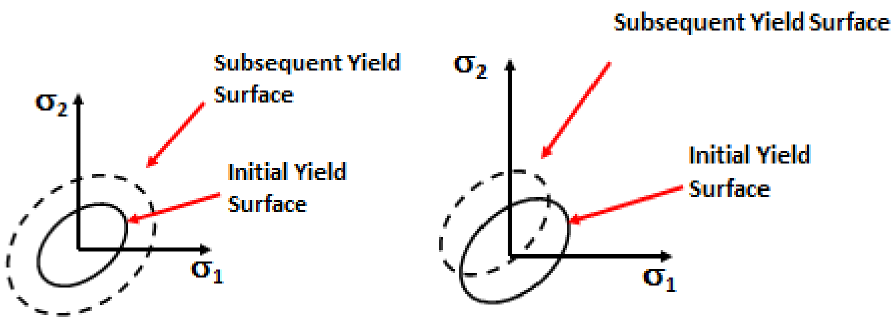

Figure 6: Isotropic hardening with change in yield surface and Figure.7: Kinematic hardening with translation of yield surface center axis [8].

Even if both isentropic and kinematic can be employed for hardening analysis, kinematic hardening used at small stress-strain cyclic loading for most metals. Generally kinematic hardening is used for small stress-strain cyclic loading applications.

In order to include nonlinear analysis in this work, the hardening modulus was included in ANSYS workbench on plasticity wizard. It is the slop of stress and strain beyond elastic limit. Besides the yield strength of the material is also included for modeling.

4.5 Stress life analysis approach

Although fatigue is related to cyclic or repetitive loading, the results used are based on linear static when we use ANSYS software. Even if nonlinearities may be present in the model, ANSYS fatigue analysis assumes linear behavior. Fatigue analysis is automatically performed by Simulation after a linear static solution.

The requirements for fatigue analysis are Young's Modulus and Poisson's Ratio, Mass and Density. Beside if thermal loads are present, thermal expansion coefficient and thermal conductivity are required. Mean stress effects in fatigue are usually presented as stress amplitude versus mean stress plot. For a particular given cyclic life it is usually observed that the load amplitude of the endurance limits decreases with growing mean stress or static load.

Typical Stress-Life Curve or S-N Curve that show the relationship of stress amplitude to cycles to failure plotted bellow.

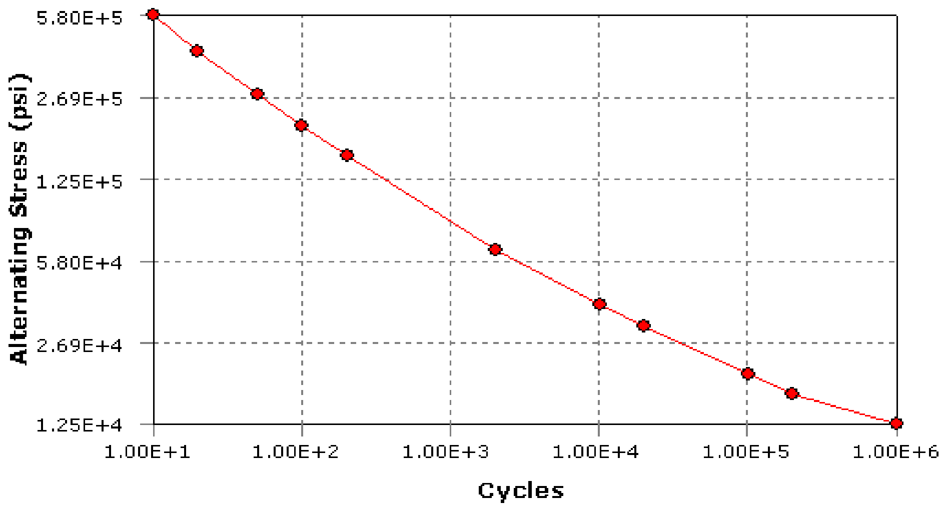

Figure 8: The Stress-Life (S-N) Curve draw to logarithmic plot

Steps implemented for the stress life analysis approach are listed in the following way:

- Attaching Geometry
- Assigning Material Properties
- Defining Contact Regions
- Defining Mesh Controls
- Including Loads and Supports
- Requesting Results, including the Fatigue Tool
- Solving the Model
- Reviewing Results

CHAPTER FIVE

ANALYSES

5.1 Mechanical load analysis

5.1.1 Contact pressure analysis

According to Hertz theory [9], the normal pressure is distributed as an ellipsoid over the elliptic contact area. The ellipsoidal normal contact pressure distribution p (x,y) is expressed By

$$P(x,y) = \frac{3W}{2\pi ab}\sqrt{(1-(\frac{x}{a})^2-(\frac{y}{b})^2)} \tag{7}$$

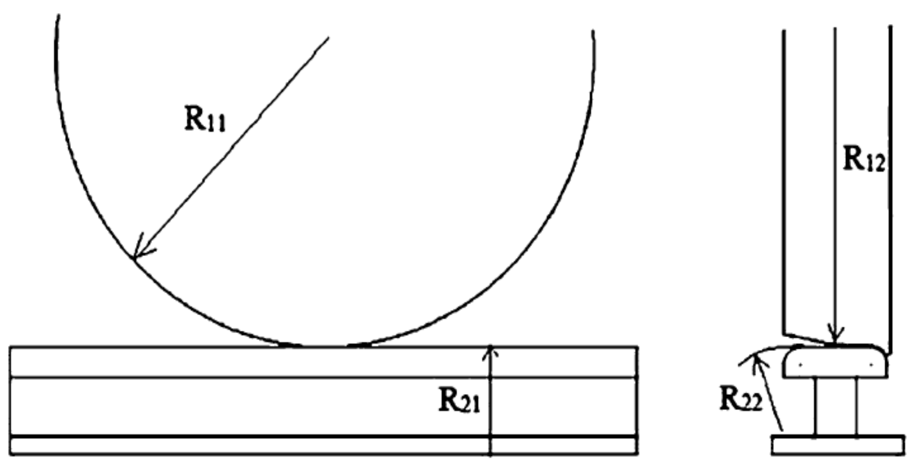

Figure 9: Wheel–rail configuration showing different principal relative radii of curvature

Radius of curvature of the wheel R11 = 420 mm,

Radius of the wheel profile R12 =∞

Rail with the radius of the head R21 = ∞

Radius of curvature of the rail in the plane of cross section R22= 300 mm

Here, a and b are the half width of the contact area in the longitudinal x and lateral y directions, respectively.in addition, E1= E2 =210Gpa is the Young's moduli of the wheel and rail materials, and ν1=ν2=0.283 are the Poisson's ratios of the wheel and rail materials

(0.3), respectively. While W is the total normal contact load for this simulation w=12,500N. To find the semi axis of ellipse first we should find the modulus k1 and k2,A,B and θ .k1 and k2 are constants that depend on the material properties of railway wheel and rail respectively, θ is the angle between the principal axes of wheel and rail, A and B are geometric parameters.k1 and k2 given by;

$$k1 = \frac{1-v_1^2}{\pi E1} \tag{8}$$

$$k1 = \frac{1-0.0.283^2}{\pi 210e9N/m} = 1.38e\text{-}12m^2/\ N$$

$$k2 = \frac{1-v_2^2}{\pi E2} \tag{9}$$

$$k2 = \frac{1-0.283^2}{\pi 210e9N/m} = 1.38e\text{-}12m^2/\ N$$

$$A + B = \frac{1}{2} * \left(\frac{1}{R11} + \frac{1}{R'12} + \frac{1}{R22} + \frac{1}{R'21}\right) \tag{10}$$

$$A + B = \frac{1}{2} * \left(\frac{1}{300mm} + \frac{1}{\infty} + \frac{1}{420} + \frac{1}{\infty}\right) = 0.00286/mm$$

$$A - B = 1/2\sqrt{\left(\frac{1}{R11} - \frac{1}{R'12}\right)^2 + \left(\frac{1}{R22} - \frac{1}{R'21}\right)^2 + 2\left(\frac{1}{R11} - \frac{1}{R12}\right)\left(\frac{1}{R22} - \frac{1}{R'21}\right)\cos(2\psi)} \tag{11}$$

Where A and B are

The angle of ψ is between the radius of the wheel and rail which is taken as $\pi/2$ for this case

$$A - B = 1/2\sqrt{\left(\frac{1}{300} - \frac{1}{\infty}\right)^2 + \left(\frac{1}{420} - \frac{1}{\infty}\right)^2 + 2\left(\frac{1}{300} - \frac{1}{\infty}\right)\left(\frac{1}{420} - \frac{1}{\infty}\right)\cos(2(\pi/2))}$$

$$= 0.000476/mm$$

$$\text{Cos}\ (\theta) = \frac{B-A}{A+B} = \frac{0.000476}{0.00286} = 0.166$$

After calculation we have the following values for A+B, A-B and θ , 0.00286 and 0.000453 and θ=80.8 respectively.

By using the following table (the Hertz coefficient) and linear interpolation method the value of m and n for the chosen rail can be easily obtained.

$\theta1$=80°, $m1$=1.128, n1=0.893, $\theta2$=85°, m 2=1.061, n2=0.944

$$m = m1 + \frac{m2-m1}{\theta2-\theta1}(\theta-\theta1) \quad (12)$$

$$m = 1.128 + \frac{1.061-1.128}{85-80}(80.8-80)$$

m =1.123

$$n = n1 + \frac{n2-n1}{\theta2-\theta1}(\theta-\theta1)$$

$$n = 0.893 + \frac{0.944-0.893}{85-80}(80.8-80)$$

n=0.897

$$a = m\sqrt[3]{(3\pi W(K1+K2))/(4(A+B))} \quad (13)$$

$$\mathrm{a} = 1.123\sqrt[3]{\frac{3\pi*12{,}500\mathrm{N}(1.38\mathrm{e}-12\mathrm{m}^2/\mathrm{N}+1.385\mathrm{e}-12\mathrm{m}^2/\mathrm{N})}{4*2.86/\mathrm{m}}} = 3.43 \text{ mm}$$

$$b = n\sqrt[3]{(3\pi W(K1+K2))/(4(A+B))} \quad (14)$$

$$\mathrm{b} = 0.897\sqrt[3]{\frac{3\pi*12{,}500\mathrm{N}(1.39\mathrm{e}-12\mathrm{m}^2/\mathrm{N}+1.39\mathrm{eN}-12\mathrm{m}^2/\mathrm{N})}{4*2.86/\mathrm{m}}} =$$

b=2.74mm

For W = 12,500N, a = 3.43 mm and 2.74 mm, the maximum pressure at the center point of the contact ellipse is given by

$$\mathrm{p(x,y)} = \frac{3\mathrm{W}}{2\pi \mathrm{ab}} = \mathrm{p(x,y)} = \frac{3*12{,}500\mathrm{N}}{2\pi*0.00343*0.00274} = 635 \text{ MPa}$$

5.1.2. Tangential load analysis

Longitudinal direction creep force that cause of large slippage on longitudinal direction during traction is considered in this case. Based on Johnson and vermulen method the resultant tangential force is approximated by [10];

$$\frac{F}{\mu N} = 1 - (1-\tau)^3 \quad \text{for } \tau = 0 \text{ to } \tau = 1 \qquad (15)$$

$$\frac{F}{\mu N} = 1 \ \text{ for } \tau > 1 \qquad (16)$$

Where μ coefficient of friction which constant have value of 0.2 for this study, F is the resultant tangential creep force, N is normal load and τ is the normalized creepage

The longitudinal normalized creepage in longitudinal direction given by

$$\tau x = \frac{(GabC11\ \xi)}{3\mu W}$$

In this equation G is modulus of rigidity, a and b are semi axis of elliptical contact N, normal load, C_{11} is kalker creep coefficient, ξ is longitudinal creepage. W=12,500N, G=82.6 G.pa,

For b/a= 0.8 and for ν= 0.5, C_{11}= 5.42, for ν= 0.25 C_{11}= 4.36

For b/a=0.8 and for ν= 0.5, C_{22}= 4.39, for ν= 0.25 C_{22}=3.99

For our case passion's ratio of steel is 0.283 by interpolation we can find the following values

$$C'11 = 4.36 + \frac{5.42 - 4.36}{0.5 - 0.25}(0.283 - 0.25) = 4.572$$

For slip velocity, 2.33, 4.55, 6.77 and 8.99 m/s the creepage values are calculated and the values are, 0.13, 0.239, 0.29, and 0.34 respectively.

The normalize creepage and longitudinal creep force each calculated as follow

For ξ=0.13, the normalize creep value will be

$$\tau x = \frac{(GabC11\ \xi)}{3\mu W} = \frac{(82.6\ Gpa * 0.00274m * 0.00343m * 4.57 * 0.13)}{3 * 0.2 * 12{,}500} = 61.49$$

Since τ > 1

The tangential force is

$$\frac{F}{\mu N} = 1$$

$F = \mu N = 0.2 * 12{,}500 = 2.5KN$

Similarly For ξ=0.239, the normalize creep value will be

$\tau x = \frac{(GabC11\ \xi)}{3\mu W} = \frac{(82.6\ Gpa*0.00274m*0.00343m*4.57*0.239)}{3*0.2*12{,}500}$=113

Since $\tau > 1$

The tangential force is

$$\frac{F}{\mu N} = 1$$

$F = \mu N = 0.2 * 12{,}500 = 2.5\ KN$

As we can notice form above calculation the normalized creep value is increasing and it is above one. For the rest of creep value we can assume the creep force will be saturated, (equals to the maximum values) which is about 2.5KN.

5.1.3 Contact stress-strain analysis due to mechanical loads

5.1.3.1 FEM solution steps for mechanical analysis

In order to find numerical results from CATIA and ANSYS workbench, the steps employed are generally summarized below

a). The models for wheel and rail are generated in CATIA V5R19. Then, after assembling the model in CATIA is imported in to ANSYS Workbench V15 as working model.

b). Modules for automatic generation of finite element models are integrated into the model in ANSYS Workbench, transient structural analysis system. Then, the generation of finite element models is accomplished for the cycle of meshing.

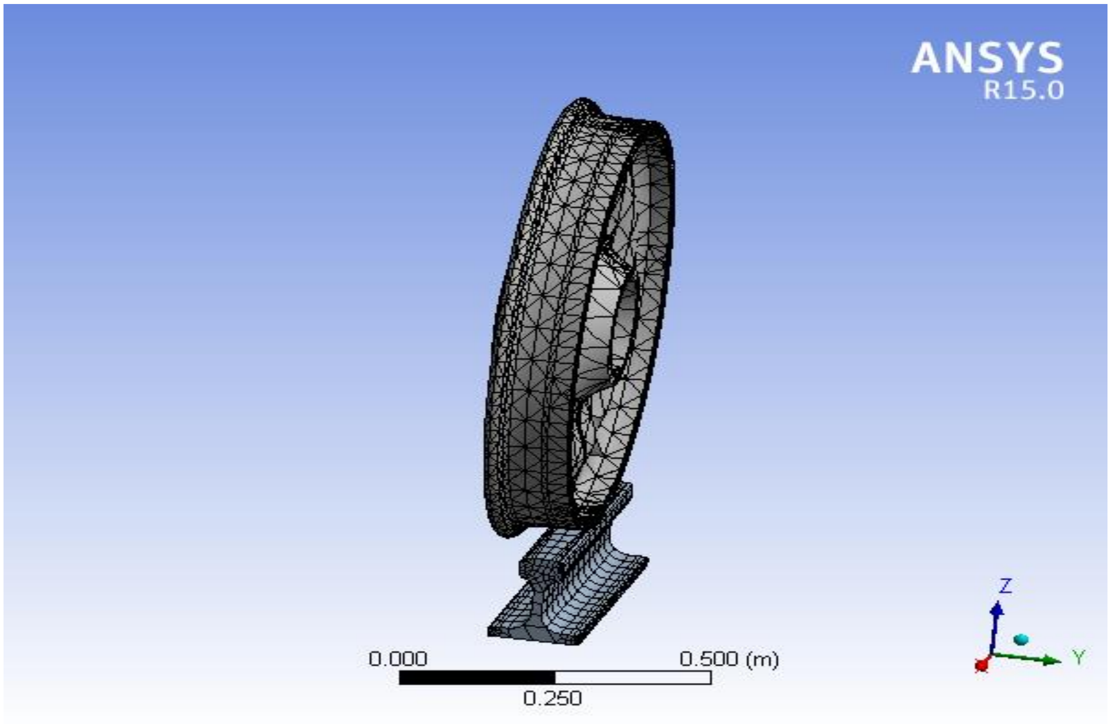

Figure 10: Mesh of rail-wheel assembly

c). Define material properties which are necessary to solve the problem. Here both the wheel and rail are carbon steel based on UIC standard with an ultimate tensile strength of 900 MPa, yield strength 600 MPa. Young's modulus of elasticity is 210 GPa.it is commonly used material which under categories of R7 steel.

d).To get the contact stresses the contact wizard is used in ANSYS Workbench. The contact algorithm in ANSYS Workbench computer program requires definition of contacting surface. To define a contact pair augmented Lagrangian method contact algorithm.

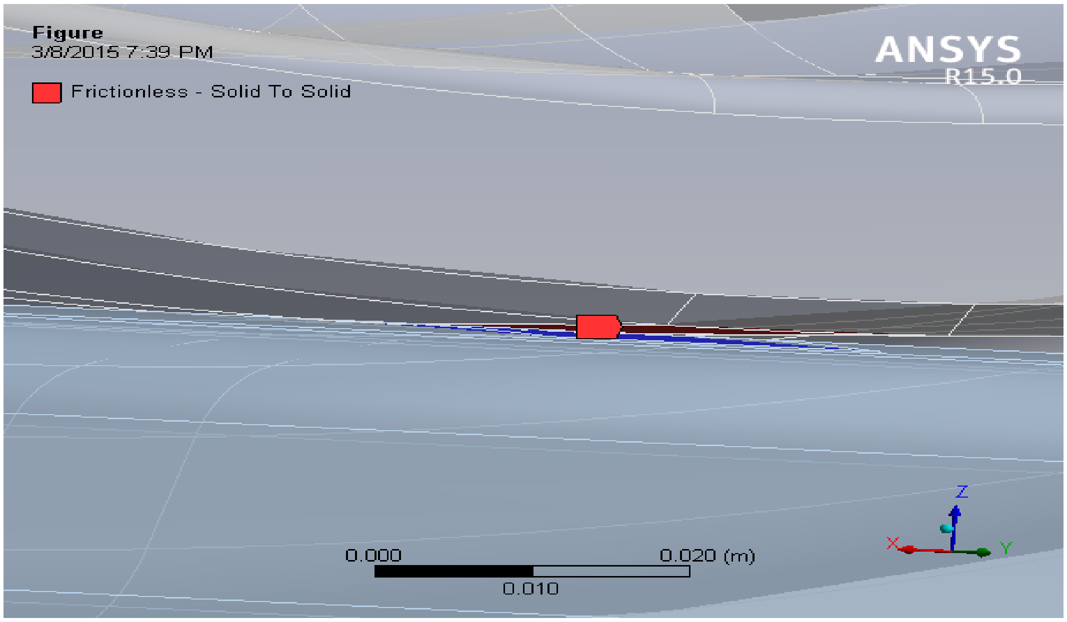

Figure 11: Rail and wheel Contact pair

e) Fixed boundary conditions (All DOF) are applied to the two area of cross section at the ends of the rail and the bottom face of the rail. As shown in the figure.

f) Wheel hub internal surfaces are selected to apply vertical load of 12.5KN and tangential load is employed at contact area having magnitude 2.5KN.

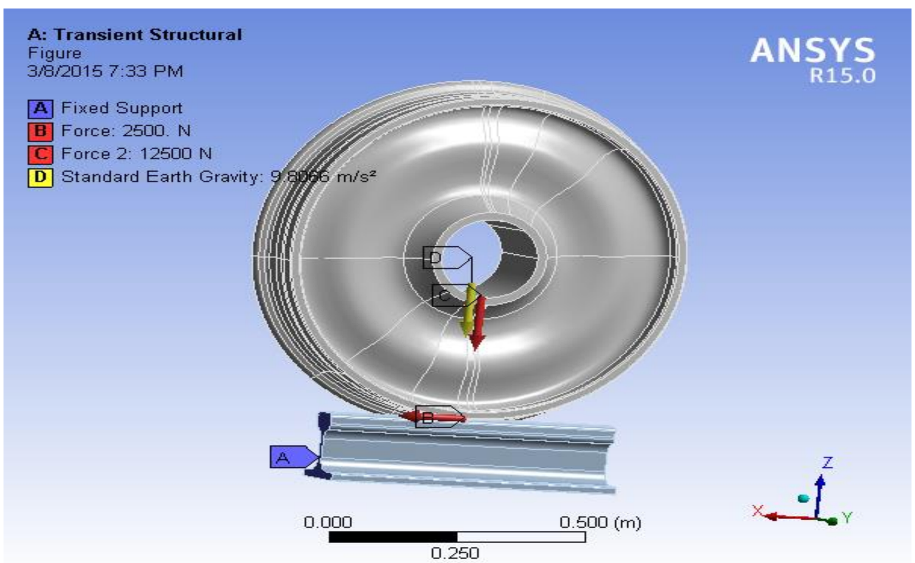

Figure 12: Boundary condition for stress-strain analysis due to mechanical load

5.2 Thermal load analysis

5.2.1 Heat flux analysis at contact area

When wheel and rail are brought into contact under the action of the static wheel load, the area of contact and the pressure distribution are usually calculated with the Hertz's theory. In this case, the area of contact is elliptical and the normal pressure distribution is [11]

$$p(x,y) = Po * \sqrt{(1 - \left(\frac{x}{a}\right)^2 - \left(\frac{y}{a}\right)^2)} \tag{17}$$

With the maximum pressure

$$Po = \frac{3N}{2\pi ab} \tag{18}$$

For the normal load N and the semi-axes a (in rolling direction) and b of the contact ellipse. In the case of a infinitely long cylinder subjected to the normal load N/b'per unit length, the normal pressure distribution is:

$$pz(x) = Po * \sqrt{(1 - \left(\frac{x}{a}\right)^2)} \tag{19}$$

With the maximum pressure

$$Po = \frac{3N}{2\pi ba\prime} \tag{20}$$

This model is often used for a simplified analysis of three-dimensional contact problems. The reference length a' for the transition from the three-dimensional to the two-dimensional case

$$a' = \frac{4}{3}.a \tag{21}$$

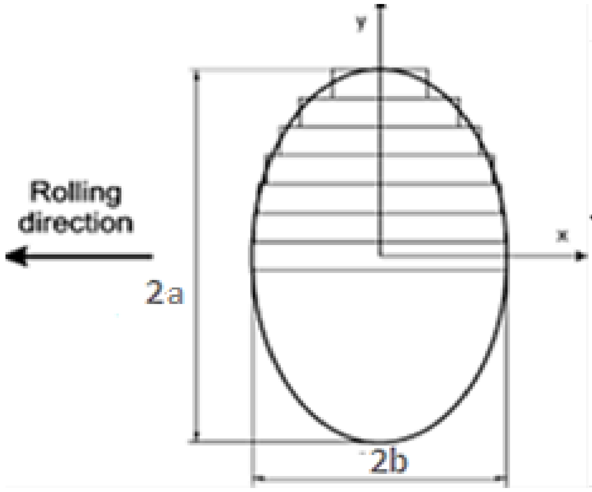

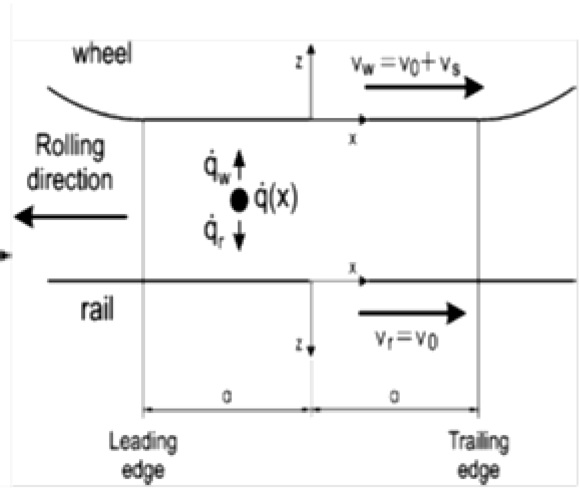

Figure 13: Elliptical area of the contact and Figure14.Co-ordinate system for temperature calculation in wheel/rail contact respectively [11]

$$a' = \frac{4}{3}.a = \frac{4}{3} * 3.43\text{mm} = 4.57\text{mm}$$

$$p._o = \frac{3N}{2\pi ba\prime} = = \frac{3*125{,}000}{2\pi*0.00274*0.00434} = 502 \text{ MPa}$$

Assuming constant values of the coefficient of friction μ=0.2 and the sliding velocity Vs, the frictional power dissipation rate in the contact patch is proportional to the pressure:

$$\phi\text{friction}(\xi) = \text{uVsPo}\sqrt{(1-\xi^2)} \quad (22)$$

It is generally assumed that all the frictional power dissipation is transformed in heat. The heat generated in the contact patch flows into the material of wheel and rail. With the heat partitioning factor ε, this can be written as

$$\phi\text{w}(\xi) = \varepsilon\phi\text{wfriction}(\xi) \quad (23)$$

$$\phi\text{r}(\xi) = (1-\varepsilon)\phi\text{wfriction}(\xi) \quad (24)$$

The surface temperatures of wheel and rail must be equal everywhere in the contact patch. The thermal penetration coefficient is given by:

$$\beta = \sqrt{\lambda\rho c} \quad (25)$$

and λ thermal conductivity heat capacity , ρ is density and assuming the rail and wheel have same interface temperature and same material property, after substituting the values we have

$$\beta = \sqrt{\lambda\rho c} = \sqrt{47.7\frac{\text{w}}{\text{m.}^{\text{o}}\text{C}} * 7850 * \frac{\text{kg}}{\text{m3}} * 480 * \text{J/kg.}^{\text{o}}\text{ C}} = 13{,}406.4$$

βw= βr =13,406.4

The part of the frictional heating that flows into the wheel is

$$\varepsilon = \frac{\beta w\sqrt{Vw}}{\beta w\sqrt{Vw}+\beta r\sqrt{Vo}} = \qquad (26)$$

ε is the heat partitioning coefficient. βr is thermal penetration coefficient of rail, Vw wheel speed . βw is thermal penetration coefficient of wheel, Vo vehicle forward speed .

For vehicle speed of V_o= 33.4 m/s and for slip velocity of 2.33 m/s the heat partitioning coefficient will be

$$\varepsilon_{\cdot 1} = \frac{\beta w\sqrt{Vw}}{\beta w\sqrt{Vw}+\beta r\sqrt{Vo}} = \frac{13{,}406.4*\sqrt{35.73m/s}}{13{,}406.4\sqrt{35.73m/s}+13{,}406.4\sqrt{33.4m/s}} = 0.5$$

The average heat flow rate at the surface of the rail is calculated in the following formula

$$\phi_{\cdot r}\,(\xi) = \frac{\pi}{4}\varepsilon_{\cdot 1}\,\mu VsPo \qquad (27)$$

$$\phi_{\cdot r}\,(\xi) = \frac{\pi}{4}\varepsilon_{\cdot 1}\,\mu VsPo = \frac{\pi}{4} * 0.5 * 0.2 * 2.33 * 502 \text{ MPa} = 92.6 \text{ MW/m}^2$$

The average heat flow rate at the surface of the wheel will be

$$\phi_{\cdot w}\,(\xi) = (1-\varepsilon_{\cdot 1})\frac{\pi}{4}\,\mu VsPo \qquad (28)$$

$$\phi_{\cdot w}\,(\xi) = (1-\varepsilon_{\cdot 1})\frac{\pi}{4}\,\mu VsPo = 0.5\frac{\pi}{4} * 0.2 * 2.33 * 502 \text{ MPa} = 92.6 \text{ MW/m}^2$$

Analysis of Heat flux and temperature at the contact area for vehicle speed of Vo= 33.4 m/s and slip velocity of 4.55 m/s

Heat partitioning coefficient;

$$\varepsilon_{\cdot 2} = \frac{\beta w\sqrt{Vw}}{\beta w\sqrt{Vw}+\beta r\sqrt{Vo}} = \frac{13{,}406.4*\sqrt{37.95m/s}}{13{,}406.4\sqrt{37.95m/s}+13{,}406.4\sqrt{33.4m/s}} = 0.52$$

The average heat flow rate at the surface of the rail;

$$\phi_{\cdot r}\,(\xi) = \frac{\pi}{4}\varepsilon_{\cdot 2}\,\mu VsPo = \frac{\pi}{4} * 0.52 * 0.2 * 4.55\frac{m}{s} * 502 \text{ MPa} = 186.5 \text{ MW/m}^2$$

The average heat flow rate at the surface of the wheel;

$$\phi_{\cdot w}\,(\xi) = (1-\varepsilon_{\cdot 2})\frac{\pi}{4}uVsPo = \frac{\pi}{4} * 0.48 * 0.2 * 4.55\frac{m}{s} * 502 \text{ MPa} = 172.2 \text{ MW/m}^2$$

Analysis of heat flux at the contact area for vehicle speed of V= 33.4 m/s and slip velocity of 6.77 m/**s**

The heat partitioning coefficient is

$$\varepsilon._3 = \frac{\beta w\sqrt{Vw}}{\beta w\sqrt{Vw}+\beta r\sqrt{Vo}} = \frac{13{,}406.4\sqrt{40.17m/s}}{13{,}406.4\sqrt{40.17m/s}+13{,}406.4\sqrt{33.4m/s}} = 0.522$$

With the average heat flow rate at the surface of the rail

$\phi._r\,(\xi) = \frac{\pi}{4}\varepsilon._3\ \mu VsPo = \frac{\pi}{4}0.522 * 0.2 * 6.77\frac{m}{s} * 502$ MPa=278.6 MW/m^2

With the average heat flow rate at the surface of the wheel

$\phi._w\,(\xi) = (1-\varepsilon._3)\frac{\pi}{4}\mu VsPo = \frac{\pi}{4}0.478 * 0.2 * 6.77\frac{m}{s} * 502$ MPa=255.1 MW/m^2

Analysis of Heat flux at the contact area for vehicle speed of Vo= 33.4 m/s and slip velocity of 8.99 m/s

The heat partitioning coefficient is

$$\varepsilon._4 = \frac{\beta w\sqrt{Vw}}{\beta w\sqrt{Vw}+\beta r\sqrt{Vo}} = \frac{13{,}406.4\sqrt{42.3m/s}}{13{,}406.4\sqrt{42.3m/s}+13{,}406.4\sqrt{33.4m/s}} = 0.53$$

With the average heat flow rate at the surface of the rail

$\phi._r = \frac{\pi}{4}\varepsilon._4\ \mu VsPo = \frac{\pi}{4}0.53 * 0.2 * 8.99\frac{m}{s} * 502$ MPa=375.7 MW/m^2

With the average heat flow rate at the surface of the wheel

$\phi._w = (1-\varepsilon._4)\frac{\pi}{4}\mu VsPo = \frac{\pi}{4}0.47 * 0.2 * 8.99\frac{m}{s} * 502$ MPa =333.18 MW/m^2

5.2.2 Temperature rise analysis at contact area

It is difficult to measure the temperature of the wheel-rail contact as mentioned earlier, theoretical predictions of temperature rise for various wheel loads, vehicle speed and slip speed are necessary. The theory is essentially that of heat flow problem involving moving sources of heat. When traction and braking forces are exerted during normal rolling, the temperature at the rolling contact will rise owing to the creep of the wheel over the rail. Although slip conditions during creep are not simply defined, the calculation is extended to determine the temperature rise when a rolling wheel is just about to undergo gross slipping due to traction or braking forces. Based on this temperature rise over contact area for different slip velocity is calculated as bellow.

Assuming that the only source of heat over the area is friction, friction-induced temperature of rail is given by

$$\Theta._r\, rmax = \frac{1.253\varepsilon._1\mu VsPo}{\beta r}.\sqrt{\frac{b}{Vr}}. \qquad (29)$$

Where μ friction is efficient, Vs is slip velocity, βr is thermal penetration coefficient of rail, $\varepsilon._1$ and is heat partitioning coefficient.

For the slip velocity of 2.33m/s the surface temperature of the rail over contact area can be calculated as

$$\Theta._r\max = \frac{1.253\varepsilon._1\mu VsPo}{\beta r}.\sqrt{\frac{b}{Vr}}.=\frac{1.253*0.5*0.2*2.33\frac{m}{s}*502\ MPa*}{13{,}406.4}.\sqrt{\frac{0.00274}{33.4m/s}} = 100^oC$$

and the friction-induced temperature of wheel is

$$\Theta._w\max = \frac{1.253\varepsilon._1\mu VsPo}{\beta w}.\sqrt{\frac{b}{Vw}}. \tag{30}$$

$$\Theta._w\max\frac{1.253\varepsilon._1\mu VsPo}{\beta w}.\sqrt{\frac{b}{Vw}}.=\frac{1.253*0.5*0.2*2.33\frac{m}{s}*502\ MPa*}{13{,}406.4}.\sqrt{\frac{0.00274}{35.73\ m/s}}=96.52\,^oC$$

With similar procedure the surface temperature over the contact area are calculated for 4.55, 6.77, and 8.99m/s slip velocities for vehicle running 33.4 m/s. The analysis is carried as follow;

Friction-induced temperatures of rail at 4.55m/s slip velocity

$$\Theta r\max = \frac{1.253\varepsilon._2\mu VsPo}{\beta r}.\sqrt{\frac{b}{Vr}}.=\frac{1.253*0.52*0.2*4.55\frac{m}{s}*502\ MPa*}{13{,}406.4}.\sqrt{\frac{0.00274}{33.4/s}}=200.3\,^oC$$

Similarly friction-induced temperature of wheel at the same slip velocity

$$\Theta._w\max\frac{1.253\varepsilon._2\mu VsPo}{\beta w}.\sqrt{\frac{b}{Vw}}.=\frac{1.253*0.48*0.2*4.55\frac{m}{s}*502\ MPa*}{13{,}406.4}.\sqrt{\frac{0.00274}{37.95\ m/s}}=174.13\,^oC$$

As we can noted from above two calculations the surface temperature of the rail is high than that of wheel surface for same slip velocity as noted in heat flux analysis case.

Analysis of friction induced temperature of rail surface at 6.77 m/s slip velocity:

$$\Theta._r\max = \frac{1.253\varepsilon._3\mu VsPo}{\beta r}.\sqrt{\frac{b}{Vr}}.=\frac{1.253*0.522*0.2*6.77\frac{m}{s}*502\ MPa}{13{,}406.4}.\sqrt{\frac{0.00274}{33.4}}.=300\,^oC$$

Friction-induced temperatures of wheel at 6.77m/s slip velocity

$$\Theta._w\max = \frac{1.253\varepsilon._3\prime uVsPo}{\beta w}\sqrt{\frac{b}{Vw}}.=\frac{1.253*0.478*0.2*6.77\frac{m}{s}*502\ MPa}{13{,}406.4}\sqrt{\frac{0.00274}{40.17\ m/s}}.=250\,^oC$$

Similarly for 8.99 m/s slip velocity friction-induced temperature of rail is

$$\Theta._{r}\max = \frac{1.253\varepsilon._{4}\mu VsPo}{\beta r}.\sqrt{\frac{b}{Vr}}.=\frac{1.253*0.53*0.2*8.99\frac{m}{s}*502\text{ MPa}}{13{,}406.4}.\sqrt{\frac{0.00274}{33.4m/s}}.=400\,^{o}C$$

and the temperature of wheel will be

$$\Theta._{w} = \max\frac{1.253\varepsilon._{4}\mu VsPo}{\beta w}.\sqrt{\frac{b}{Vw}}.=\frac{1.253*0.47*0.2*8.99\frac{m}{s}*502\text{ MPa}}{13{,}406.4}.\sqrt{\frac{0.00274}{42.3\text{ m/s}}}.=315.9\,^{o}C$$

Surface temperatures greater than 400 ^{o}C can be noted in similar calculation for high slip velocity.

5.2.3 Comparison with Heat flux and contact temperature during barking

During barking the velocity of rail will be V_r and velocity of wheel will be $V_w=V+V_S$ where V is vehicle forward speed and V_S is slip velocity. For my study V=33.34 m/s and Vs are 2.33, 4.55, 6.77, 8.99 m/s. When we compare contact temperature at 2.33 m/s during traction and barking analytically. Assuming equal heat partitioning coefficient between rail and wheel the maximum surface temperature at contact area will be $\frac{1.253*0.5*0.2*2.33\frac{m}{s}*502\text{ MPa}}{13{,}406.4}.\sqrt{\frac{0.00274}{31.07\text{ m/s}}}.$ =104, high value of contact temperature is estimated through analytical analysis but contact pressure and tangential load are remain the same.

5.2.4 Contact Stress-stain analysis due to thermal load

5.2.4.1 FEM solution steps for thermal analysis

a).Similar to analysis for mechanical loads, the models for wheel and rail are generated in CATIA V5R19. Then, after assembling the model in CATIA is imported in to ANSYS Workbench V15.0 as working model.

b).Modules for automatic generation of finite element models are integrated into the model in ANSYS Workbench version 15.0, transient thermal analysis system. Then, the generation of finite element models is accomplished for the cycle of meshing.

c).Define material properties which are necessary to solve thermal problems. Conductivity, specific heat, thermal expansion coefficient and density should introduce.

d).The contact pair is also created using augmented lagrangian method with symmetric behavior.

e).Thermal load over the contact area is applied which is surface temperature. The temperature of rail and wheel is vary for the four case of analysis i.e surface temperature of rail 100 ^oC,200 ^oC,300 ^oC,400 ^oC the respective temperature of wheel applied according to analytical result.

f).The temperature distribution over surface of contact is assumed uniformly distributed .the conduction and convection heat transfer through the bodies of rail and wheel is allowed

g).The result of transient thermal analysis is transfer to transient structural analysis. With the only load applied is contact area temperature and solved to get thermal stress and strain at contact. The load is applied for average time of 0.16 micro second, time require crossing contact area constant speed.

5.3. Simulation of combined thermo-mechanical load effect at contact area

5.3.1 Temperature dependent property of the materials

For this simulation carbon Steel is used for wheel and rails materials having ideally identical property and elasticity modulus and Poisson's ratio values are E1 = E2 = 210 GPa, and $\nu_1 = \nu_2$= 0.283, and σ_y= 600Mpa, σ_{ut}=900 Mpa, E_t=15 Gpa , c = 480 (J/kg-C) and α = 1.2e-5 ($^oC^{-1}$), λ= 47.7 (W/m ^oC) at normal condition. Additional temperature dependent material properties used for this study are listed below.

Table 1: Temperature dependent property of the materials used for the analysis [12]

T (°C)	ρ (kg m^{-3})	E (GPa)	ν	σ_Y (MPa)	E_t (GPa)	α (10^{-6} °C^{-1})	c (J kg^{-1} °C^{-1})	λ (W m^{-1} °C^{-1})
100	7818	203.8	0.2860	560.0	15.00	12.20	487.5	47.10
200	7785	197.5	0.2900	550.0	15.00	12.80	525.0	45.30
300	7753	191.3	0.2940	540.0	13.50	13.40	575.0	43.00
400	7720	185.0	0.2980	530.0	12.00	14.00	625.0	40.00

Where T is contact temperature, ρ is density E is young's modulus, E_t is hardening modulus ,υ poison's ratio, σ_Y is yield strength , α thermal expansion coefficient c heat capacity and λ is conductivity

For combined load analysis we have four loading condition. For each case the corresponding temperature dependent mechanical and thermal property is included in ANSYS workbench. One row of material properties is used at once in order to see the material response on load in that situation rather than coding entire property to simulation.an example of setting carbon steel material data for 100 ^{o}C surface temperature combined load analysis is annexed to end of this paper.

5.3.2 Boundary condition for combined load simulation

In order to build a realistic model of wheel/rail contact problem a 3D elastic-plastic finite element model is needed. This model should be able to accurately calculate the 3D stress response in the contact region as well as includes both material and geometric nonlinearity. CATIA V5 model is imported to ANSYS 15.0 workbench. Both transient thermal and structural analysis employed for the simulation. First transient thermal analysis is carried by repeating the procedure discuses in for thermal stress-strain analysis then transferred to transient structural. But now mechanical load is introduce in order to carry out combined analysis.

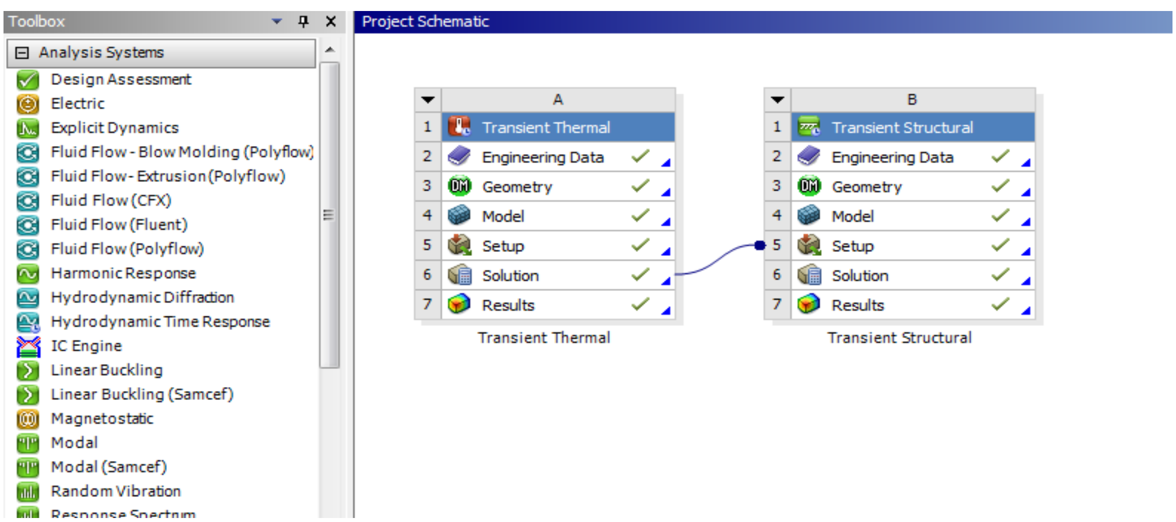

Figure 15: Ansys workbench setting for combined load case analysis

All boundary condition and loading applied based on analytical results. Fixed boundary condition is set to the rail at the bottom of the foot and the sides. The maximum pressure at the center of contact area is exerted. But all applied loads are controlled by duration of lasting. Heat that can be generating from frictional contact is applied over the contact area and tangential/translational load is applied to the center of contact region. All other necessary condition for the analysis is assumed and included like standard earth gravity.

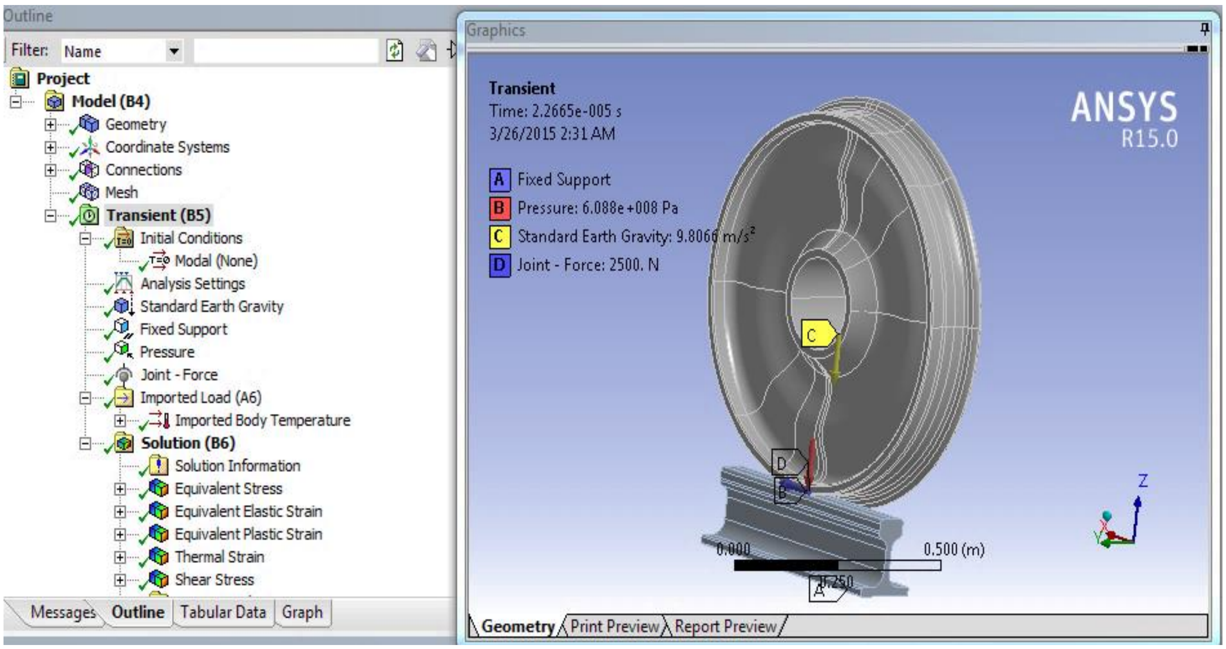

Figure 16: Mechanical load setting over imported contact surface thermal load for combined analysis

CHAPTER SIX

RESULTS AND DISCUSSIONS

6.1 Results

6.1.1 Mechanical load stress-strain analysis result

The main causes of mechanical loads are tangential and normal force. Based on analytical result the tangential force considering only longitudinal direction is 2.5KN and axle load of 25KN the distributed equally left and right wheel. Duration of applied load for simulation is the time requires crossing a contact area. The contact area is considered symmetrical. Stress, strain and stress life over contact area is presented in figures bellow.

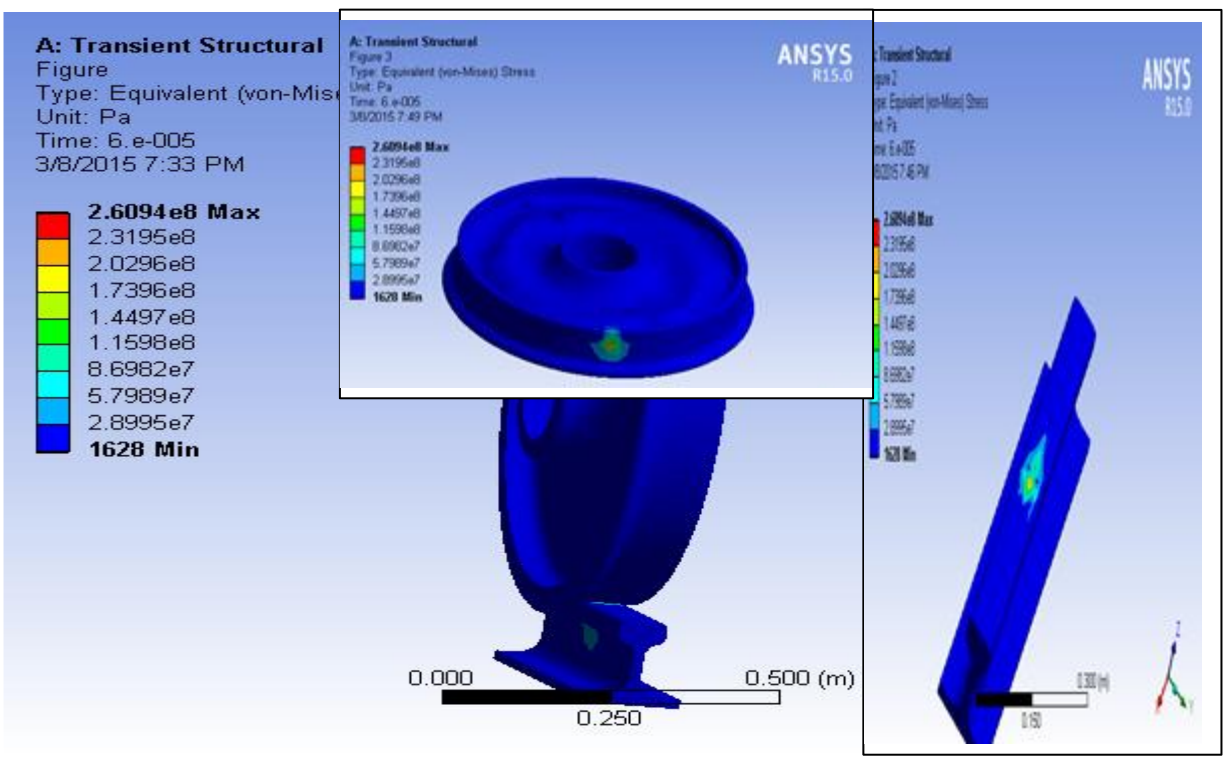

Figure 17: Stress at contact area due to mechanical load

When we check the for the safety factor it is found to be above one. Beside There is very little red spot or maximum stress point exist in contact area. Only at center of contact is noticed.

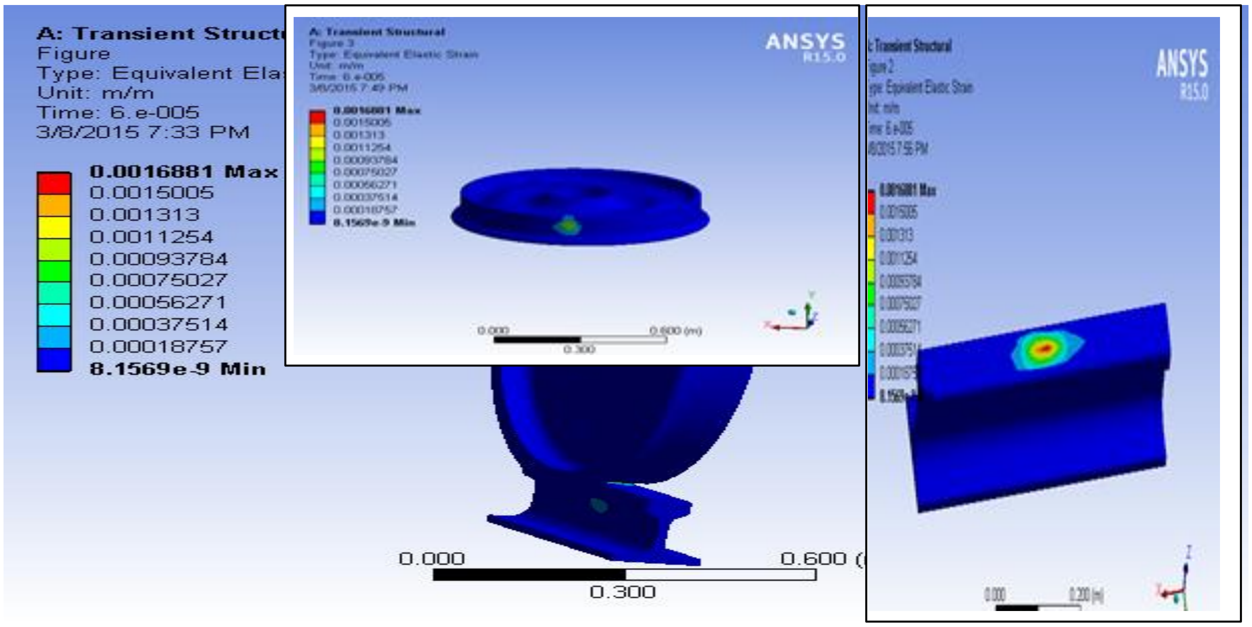

Figure 18: Elastic strain at contact area due to mechanical load

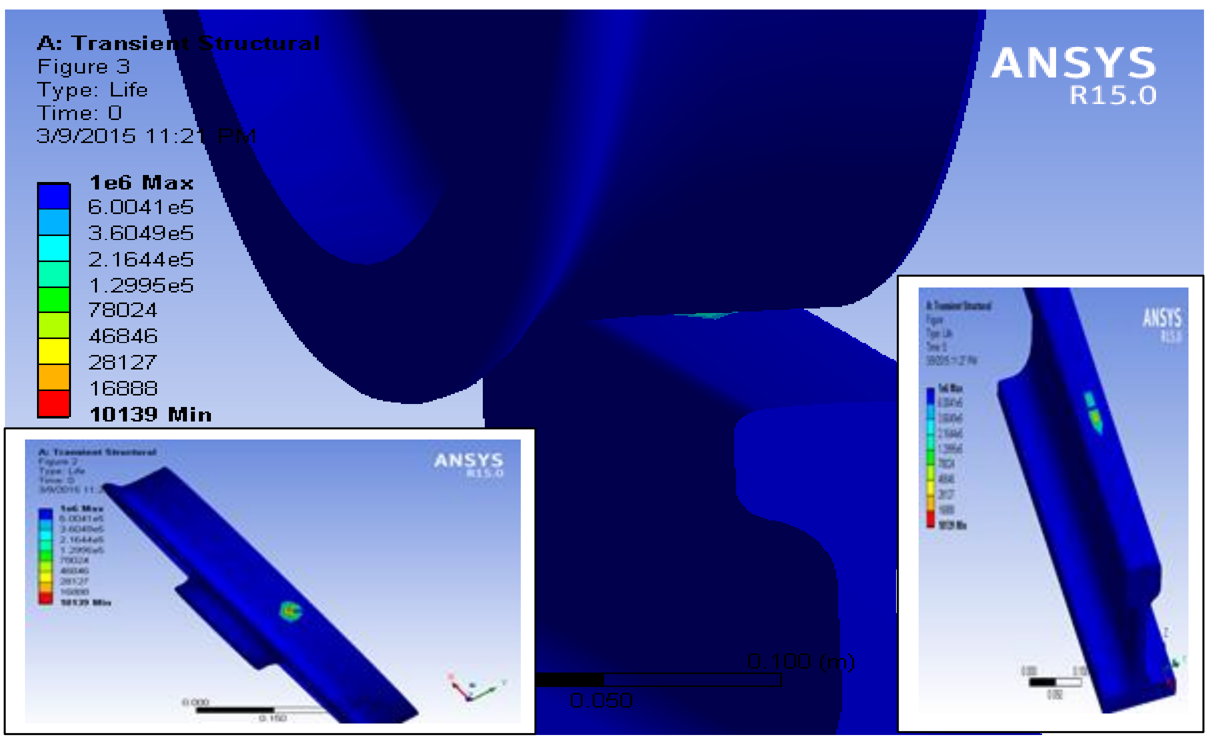

Figure 19: Contact area stress life during mechanical load only

Without considering micro structural change of contact area due to thermal load, with maximum alternating stress 2.609 MP the minimum endurance limit of the contact area will be $1.01 * 10^4$ cycle.

6.1.2 Thermal stress analysis result

The source of heat generation at the contact area between rail and wheel is friction force. The slip between wheel and rail causes frictional heating of both bodies. The maximum surface temperature during rolling contact of railway wheels with sliding friction is estimated using Blok's flash temperature formula. In addition for determining temperature rise of these components, the heat partition factor of rail and wheel is added on analysis. The results can be summarized in the following tables.

Table 2: Result summary of heat flux and max temperature at rail surface

Slip velocity (m/s)	2.33	4.55	6.77	8.99
Heat flux (M W/m^2)	92.6	186.5	278.6	375.7
Surface temperature (^{o}C)	100	200.3	300	400

Table 3: Result summary of heat flux and max temperature at wheel surface

Slip velocity (m/s)	2.33	4.55	6.77	8.99
Heat flux (M W/m^2)	92.6	172.2	255.1	333.18
Surface temperature (^{o}C)	100	174.13	250	315.9

Using the result found from temperature rise from different slip velocity analytical, finite element transient thermal stress analysis is carried out for the above surface temperature cases . During the simulation the conduction from the wheel into the rail and free convection at form all surfaces is considered. As can be noted from result bellow the thermal stress increasing highly when contact temperature is rise which contribute for thermal strain development.as high as 501Mpa thermal stress is noted from the result which near to yield strength of the materials. The results are presented in the following section.

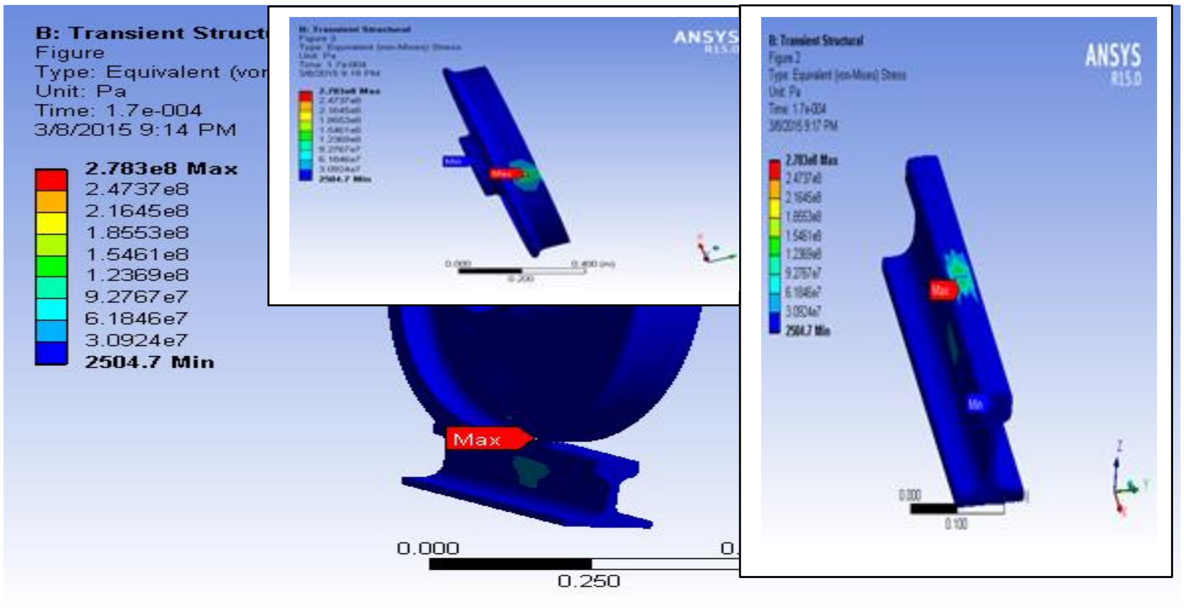

Figure 20: Contact area thermal stress for 2.33 m/s slip velocity simulation

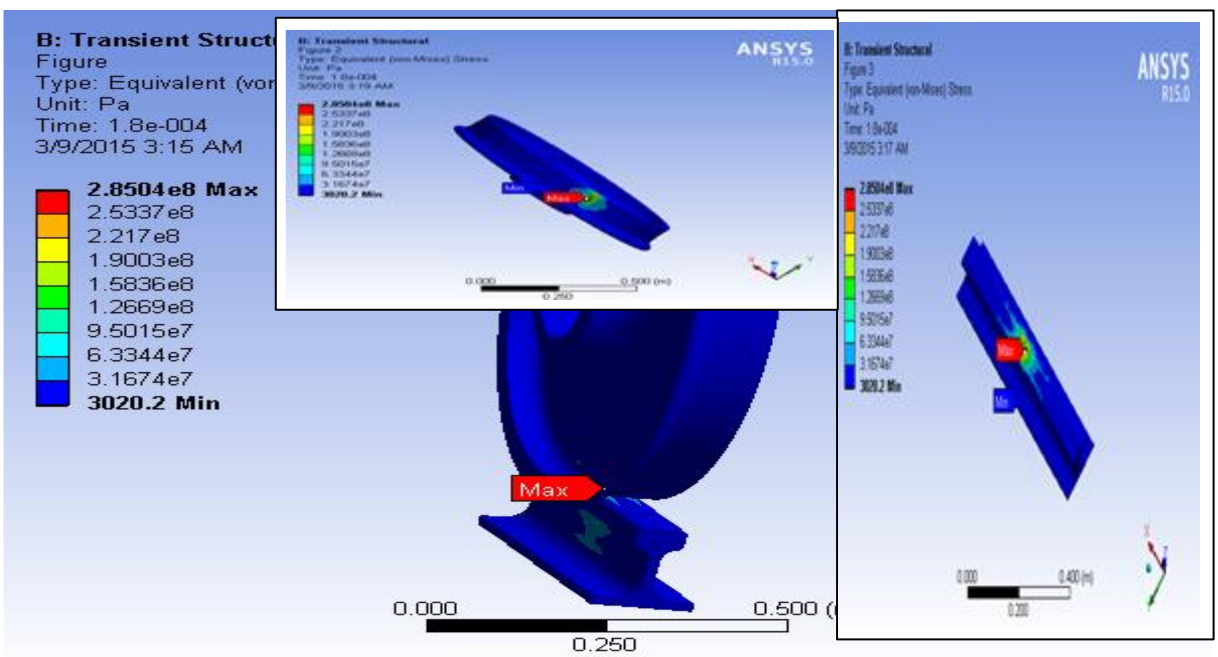

Figure 21: Contact area thermal stress for 4.55 m/s slip velocity simulation

Contact area thermal stress is zero at mechanical load only and it is about 278Mpa during combined loading when surface temperature is elevated by 100 ^{o}C the thermal stress.

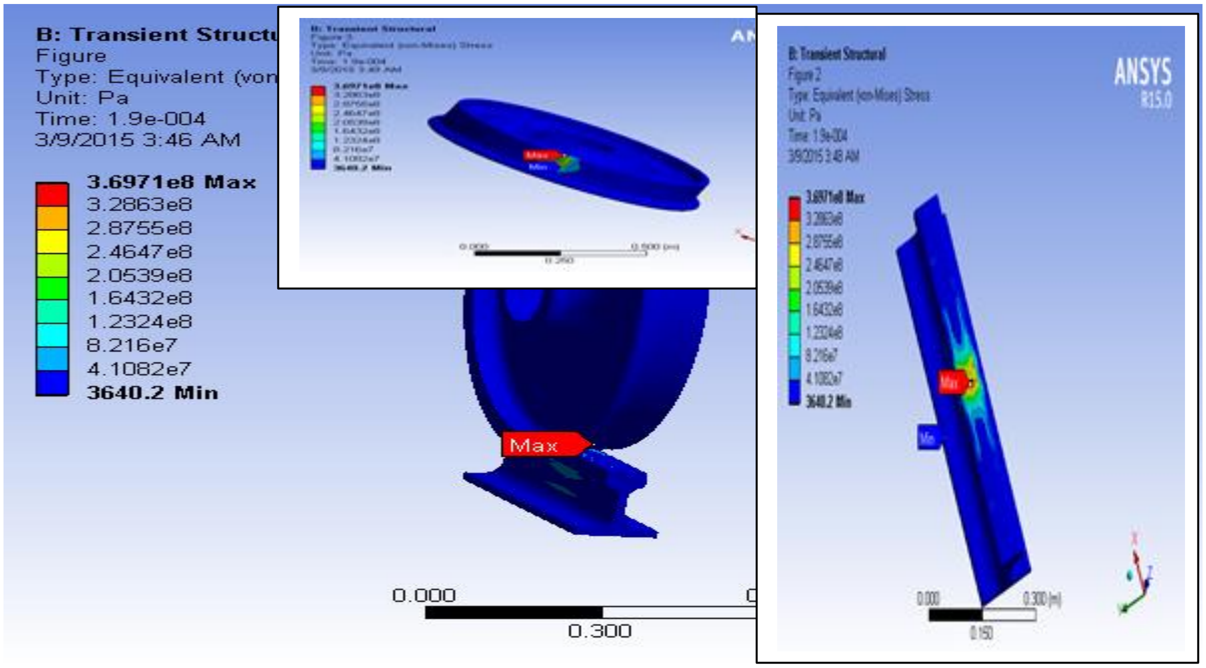

Figure 22: Contact area thermal stress for 6.77 m/s slip velocity simulation

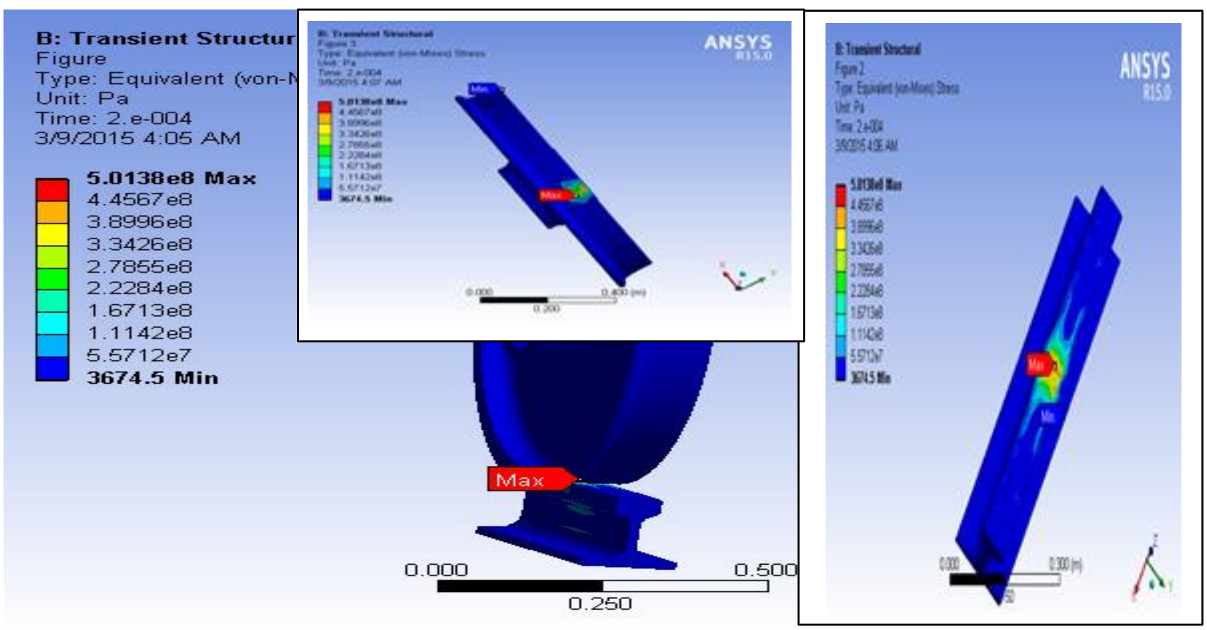

Figure 23: Contact area thermal stress for 8.99 slip velocity simulation

The only cause thermal stress on contact area is presence of thermal load. It is not possible to see thermal stress without thermal load unless friction induced load thermal or other source of heat exist in simulation.

6.1.3 Combined thermo-mechanical load effect analysis results

To calculate combined thermo-mechanical load effect on rail material, a small part of rail on which the wheel presses down on contact at different surface temperature is modeled. All loads are applied at once for specified duration of time. The axle load is divided in to wheels. This is because of straight track analysis. In addition, once frictional heating is introduced in contact area. Summary of loading condition is presented in the following table.

Table 4: Summary of loading condition for combined thermal and mechanical simulation

Slip velocity	Applied load at contact area		
	Thermal load	Mechanical loads	
	Maximum surface temperature	Normal load (pressure)	Tangential load
2.33 m/s	100 ^{o}C	635Mpa	2.5KN
4.55 m/s	200 ^{o}C	>>	>>
6.77 m/s	300 ^{o}C	>>	>>
8.99 m/s	400 ^{o}C	>>	>>

The following results are from combined mechanical and thermal load analysis over contact area for single pass. The stress life is analysis for repeated load case. Symmetric contact behavior is model and all loads are applied to the contact region. Based on the input data equivalent von mises stress, elastic strain, thermal strain, plastic strain and stress life analysis is conducted for contact surface temperature of 100,200,300,400 ^{o}C ,the results are presented pictorially in the following sections.

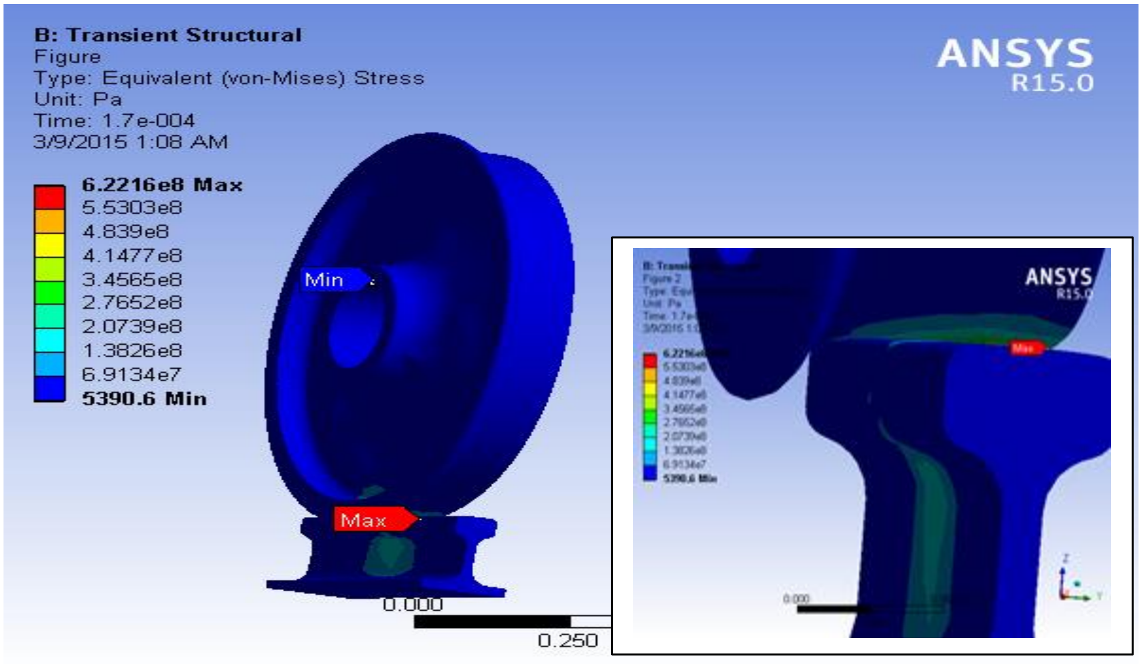

Figure 24: Equivalent von mises stress at 2.33 m/s slip velocity simulation

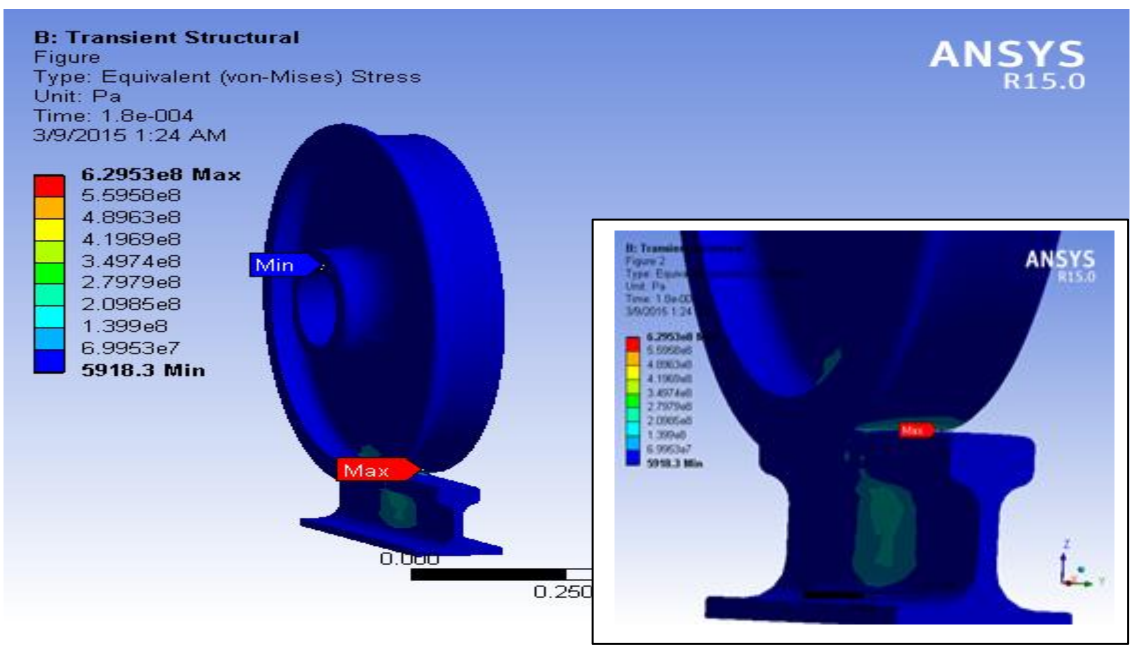

Figure 25: Equivalent von mises stress at 4.55 m/s slip velocity simulation

When we check the for the safety factor it is found to be above one. Beside There is very little red spot or maximum stress point exist in contact area. Only at center of contact is noticed.

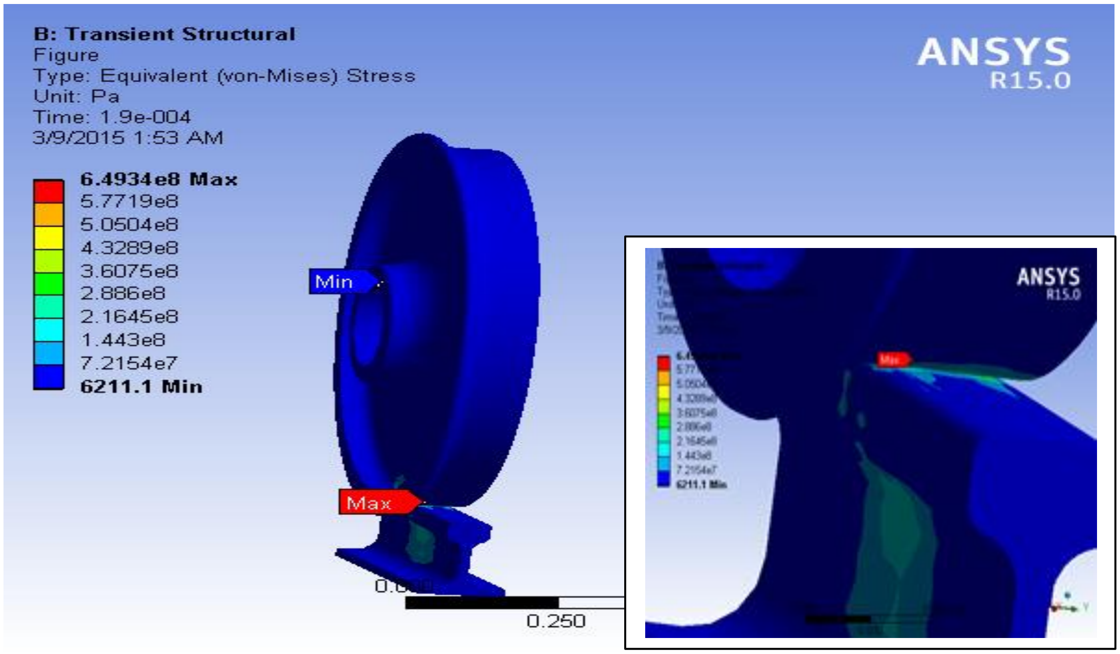

Figure 26: Equivalent von mises stress at 6.77 m/s slip velocity simulation

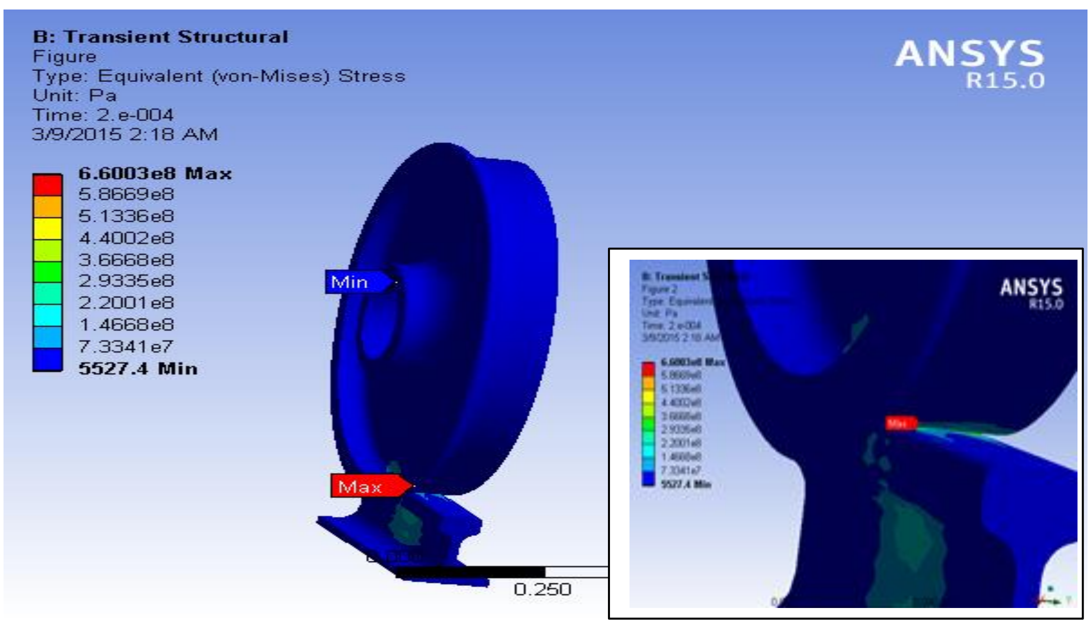

Figure 27: Equivalent von mises stress at 8.99 m/ slip velocity simulation

The equivalent von misese stresses in the four case of analysis is greater than the yield strength of material in combined load analysis. Even if critical stress points confined in few area, the existence of thermal load because of slippage affects the strength of the materials.

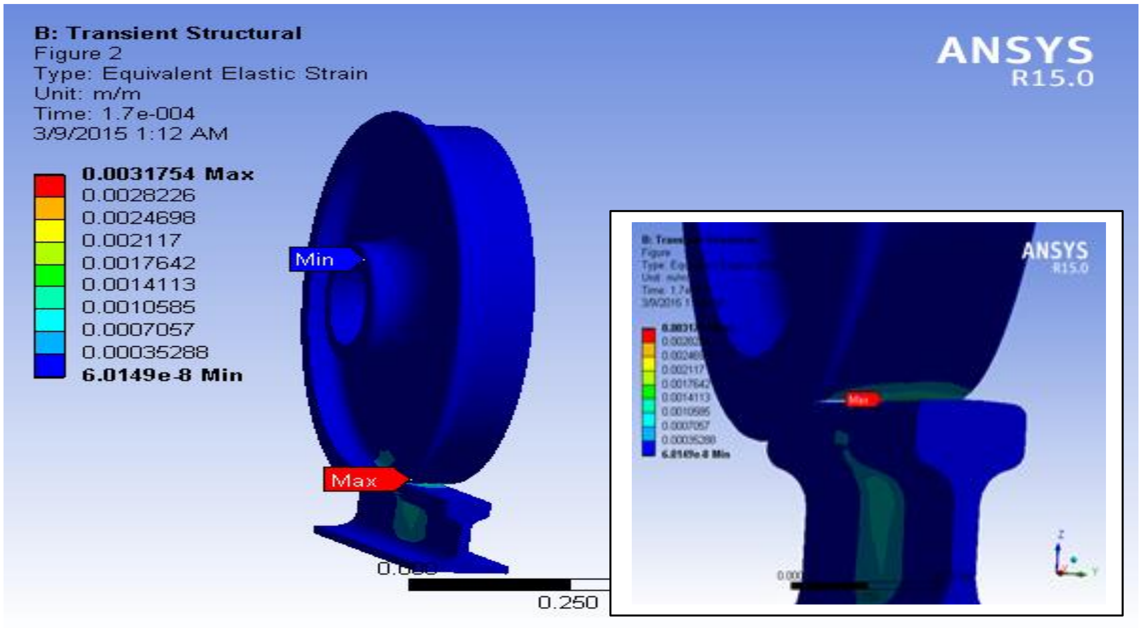

Figure 28: Elastic strain over contact area at 2.33 m/s slip velocity

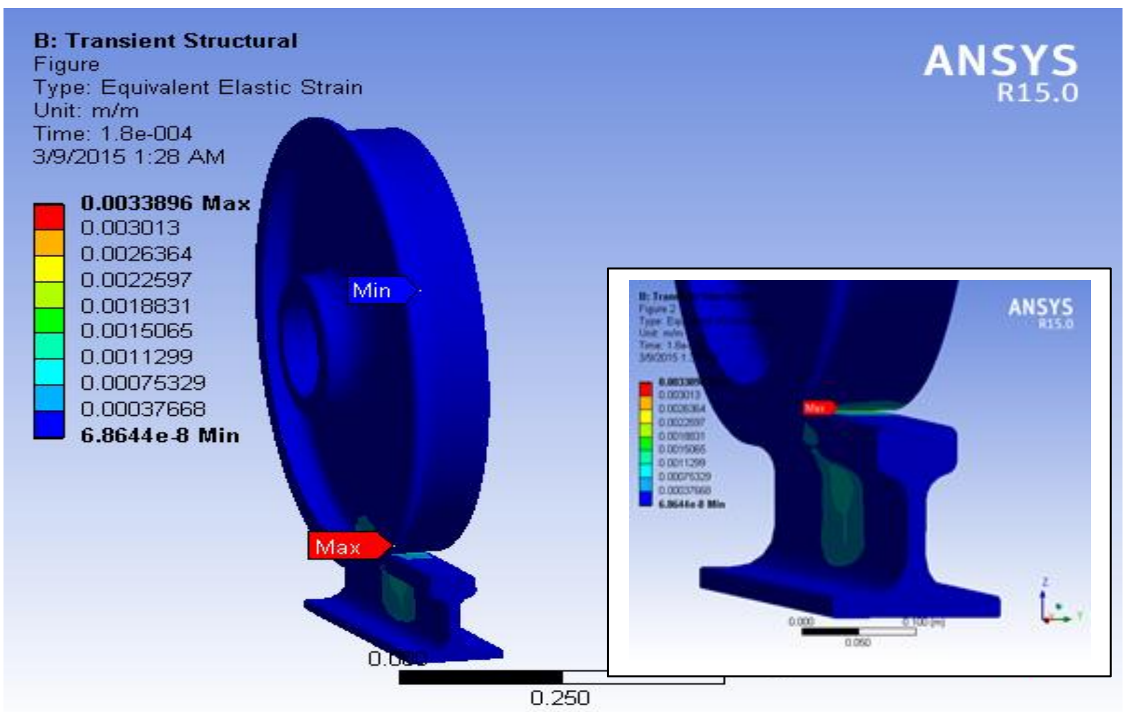

Figure 29: Elastic strain over contact area at 4.55 m/s slip velocity

Elastic strain resulted due to contact stress lower than elastic limit of the material. Most of stresses distributed over the area are lower than elastic limit except at red spot once.

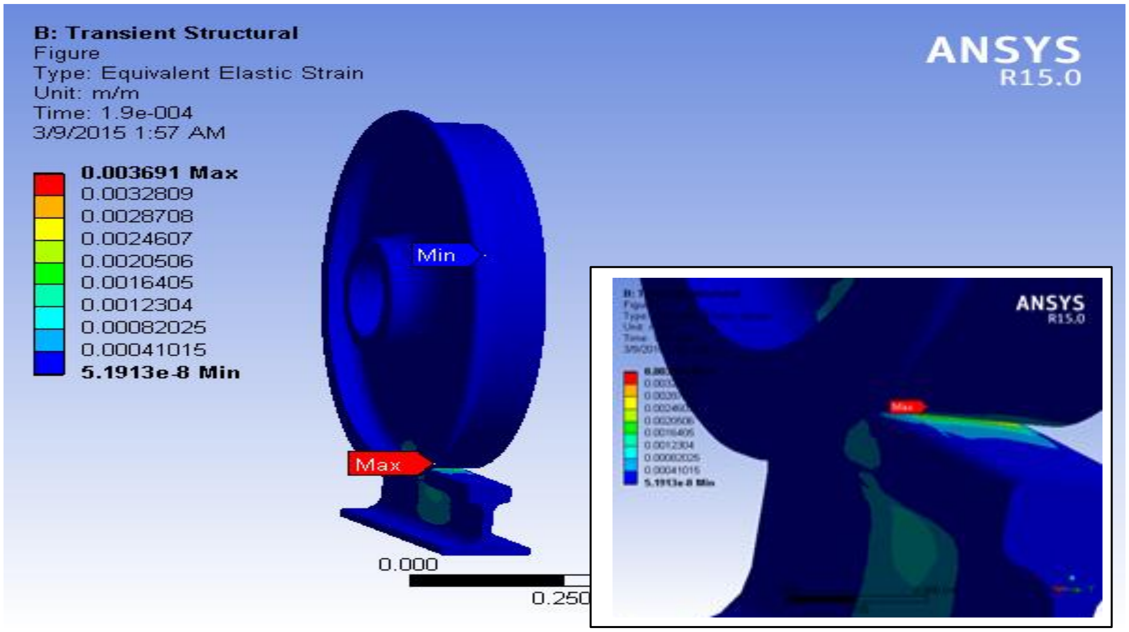

Figure 30: Elastic strains over contact area at 6.77 m/s slip velocity

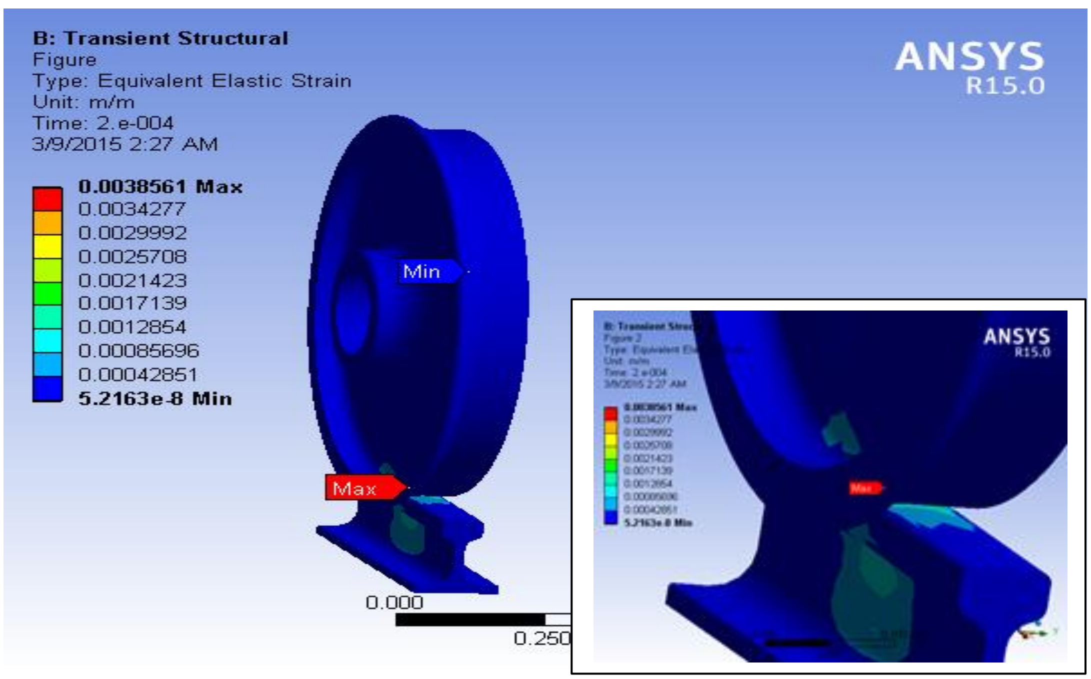

Figure 31: Elastic strains over contact area at 8.99 m/s slip velocity

Form above simulation reslut when we compare ealstic strains at contact of the four loading condition magnitud and surface area coverage of elastic strains is increase when the themal and mechanical load is incrased.

The above stress-strain analysis result indicates that the loads creat the sterss on wheel as well as the rail material.They have conducted from combied thermal and mechanical loads. According to heat partitining factor more heat is applide in to rail,so the effct is high at rail.even if the time sept for each loading case varise the combined stress and elastic starin on contact artea is increased as tempartues of the contact surface incresae.

Slippage between rail and wheel contact is not only caues stress and elastic strain,thermal stress and strain will also created on sliding areas due to friction. A few milliseconds of time the slip between wheel and rail becomes large can cause small material volumes in the contact to be heated several hundred degrees Celsius temperature. The surface temperatures greater than 1000 ^{o}C can be generated. This will cause thermal stress development on sliding contact area. As the element of area leaves the contact zone the heat input becomes zero and the surface temperature decays by conduction into the bulk material,

In the next section thremal strain and plastic strain result peresent for different loadingds. During the simulation the conduction from the wheel into the rail and free convection form all surfaces is considered.

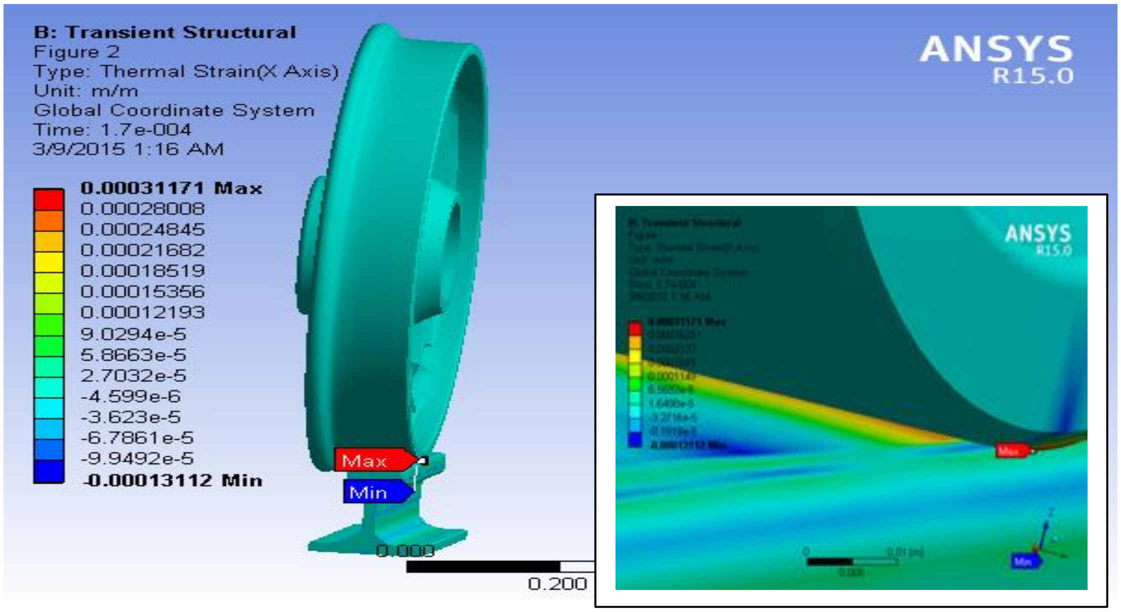

Figure 32: Thermal strain over contact area at 2.33 m/s slips velocity

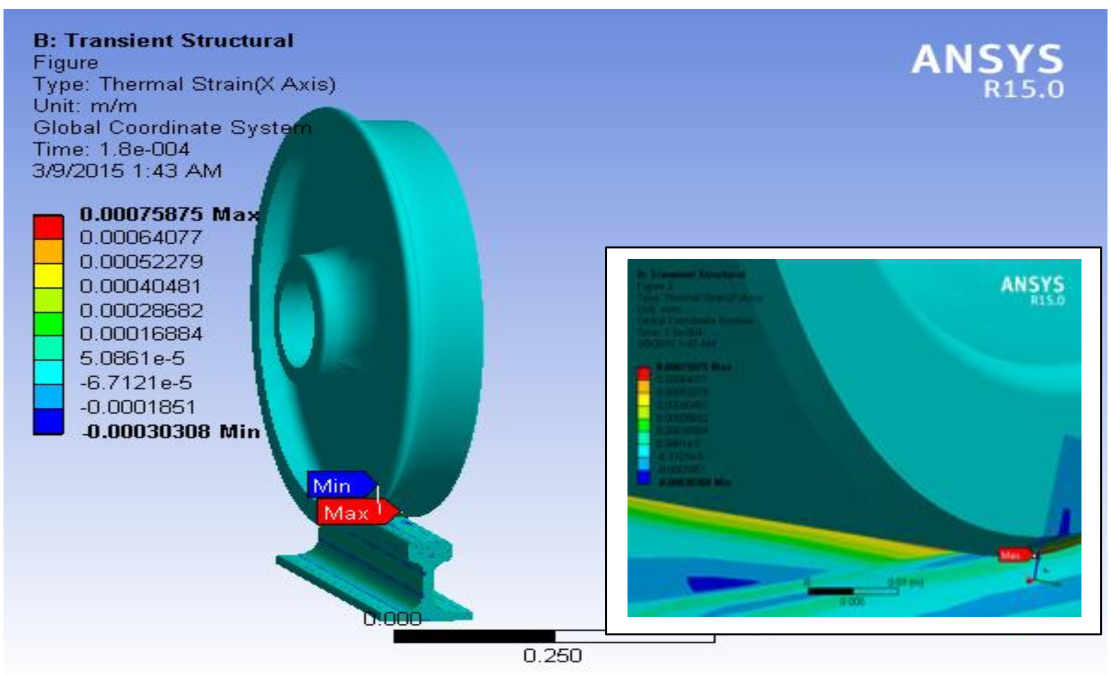

Figure 33: Thermal strain over contact area at 4.55 m/s slips velocity

From analytical result for slip velocity of 2.33 and 4.55m/s the surface temperature rise to 100 and 200 ^{o}C respectively. As surface as contact surface temperature increases the thermal strain induce also increase as can be notice from graphical results.

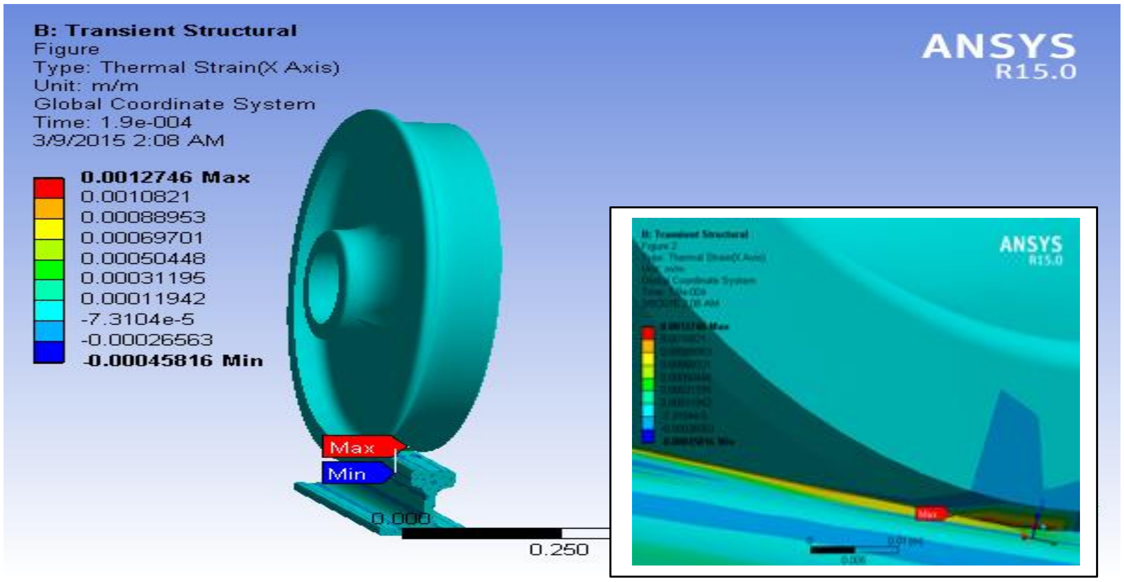

Figure 34: Thermal strain over contact area at 6.77 m/s slips velocity

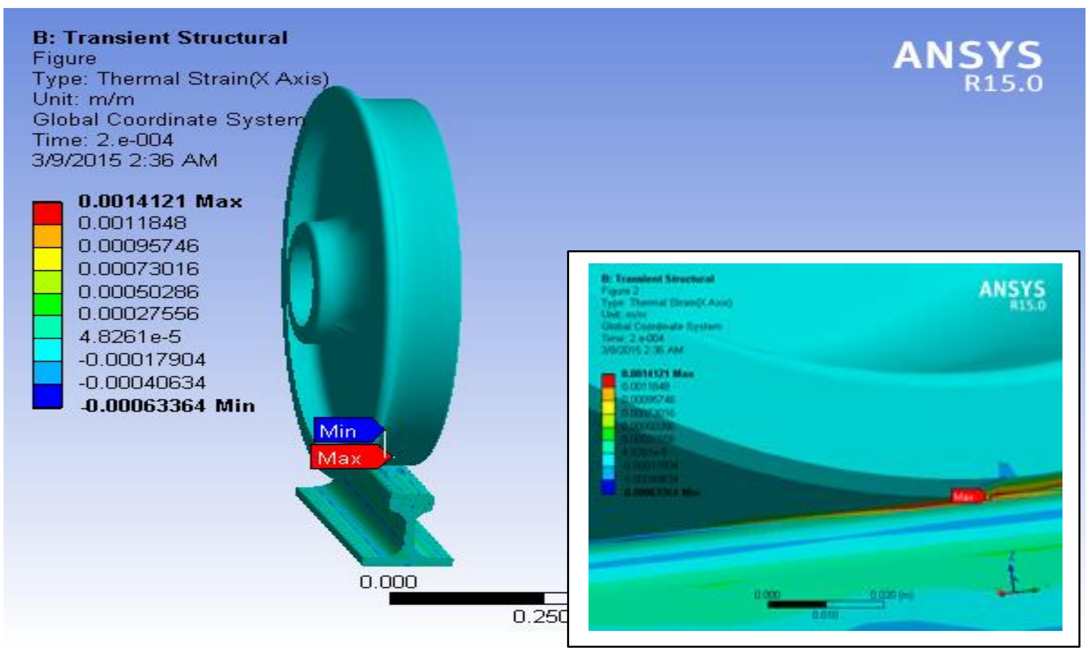

Figure 35: Thermal strain over contact area at 8.99 m/s slips velocity

Slippage result heating of both rail and wheel surface. Due to sliding of wheel in to new rail contact point ,rail surfece induced more heat that genrate by friction. In the real situation the rail is long and the thermal load will be disturbuted along length.Thefor more thermal stress and strain is accumulated on wheel surface.

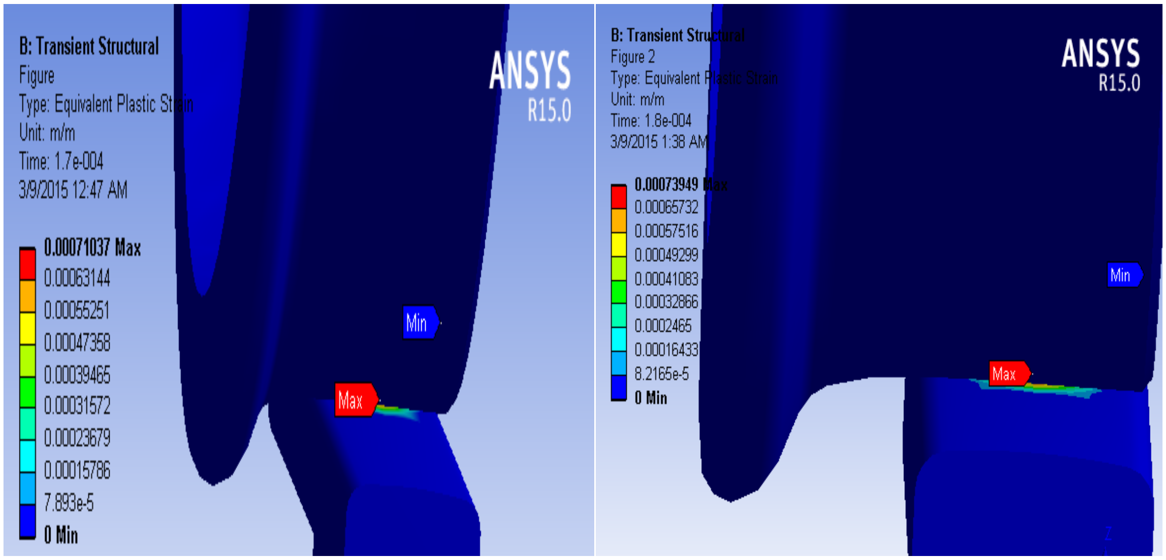

Figure 36: Plastic strain distribution over contact area at 2.33 m/s and 4.55 m/s slips velocity

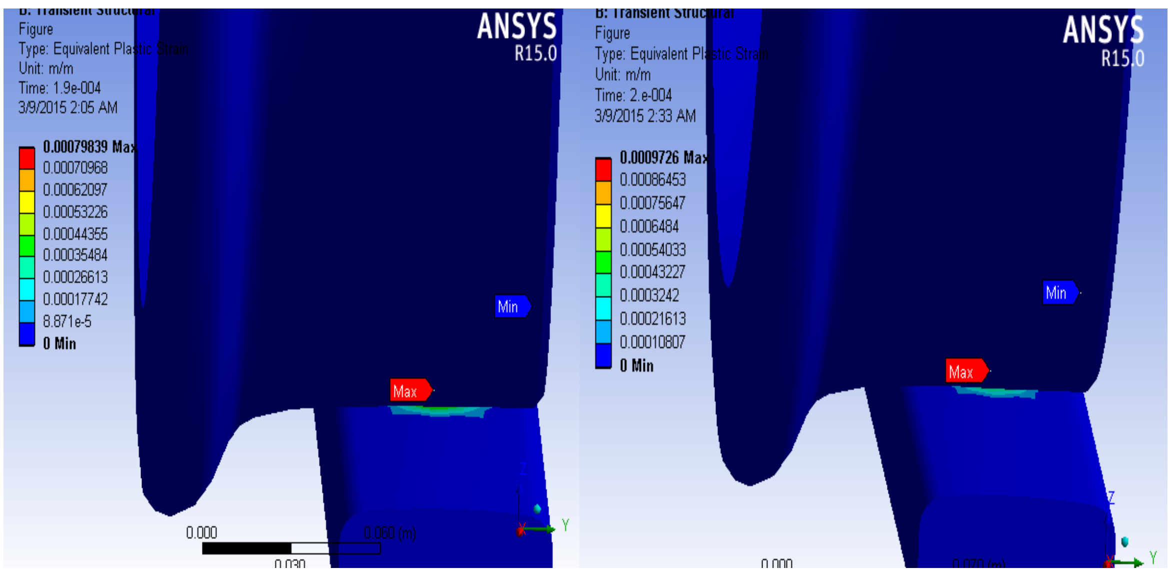

Figure 37: Plastic strain distribution over contact area at 6.77 m/s and 8.99 m/s slips velocity

In order to see the real material respons to loading at different tempratue ,including their property at different temprtaue is essential. One of the respons that alter at different temprature is plastic strain plastic strain increase with the increase of temprature.

Stress life analysis is one of indication of the effect loads on rail and wheel material. Contour plot results showing the number of cycles until failure due to fatigue.

Addtionally Gerber mean stess correction theory provides good fit for ductile metals for tensile mean stresses, although it incorrectly predicts a harmful effect of compressive mean stresses, as shown on the left side of the graph

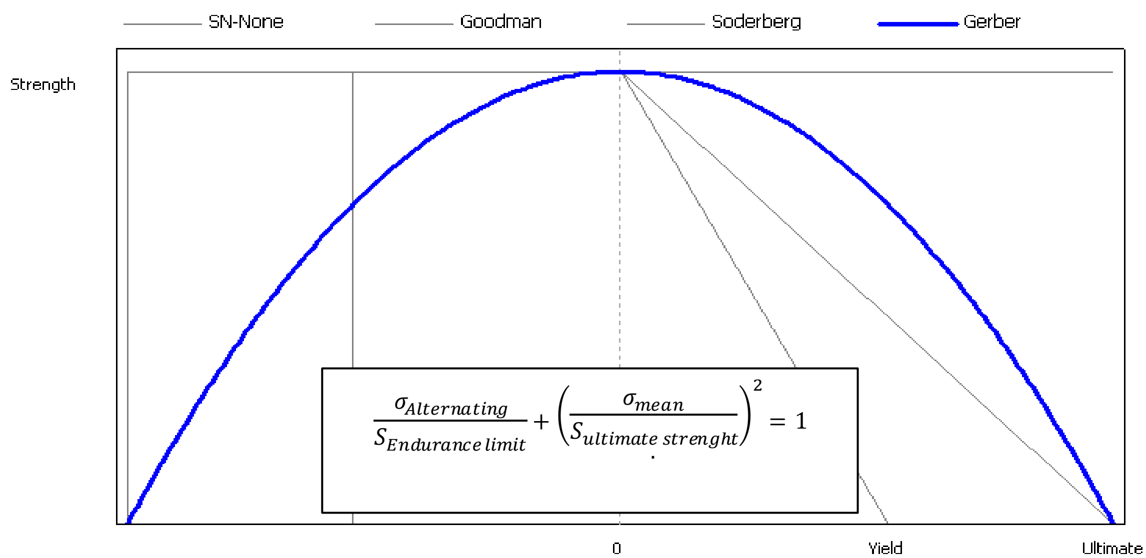

Figure 38: Equation and graphical representation of the Gerber Mean Stress Correction for Stress Life Fatigue Analysis.

The contur plot Stress life analysis over contact are for mechanical and thermal load during 2.33 m/s,4.55m/s,6.77m/s,8.99m/s slippage presnted graphcally in the next section

The fatigue analysis is performed with workbench fatigue wizard. The stress life type set with fully reversed loading. The fatigue strength factor is set to be 1. very some stress life is notice this is because of very high contact loads.

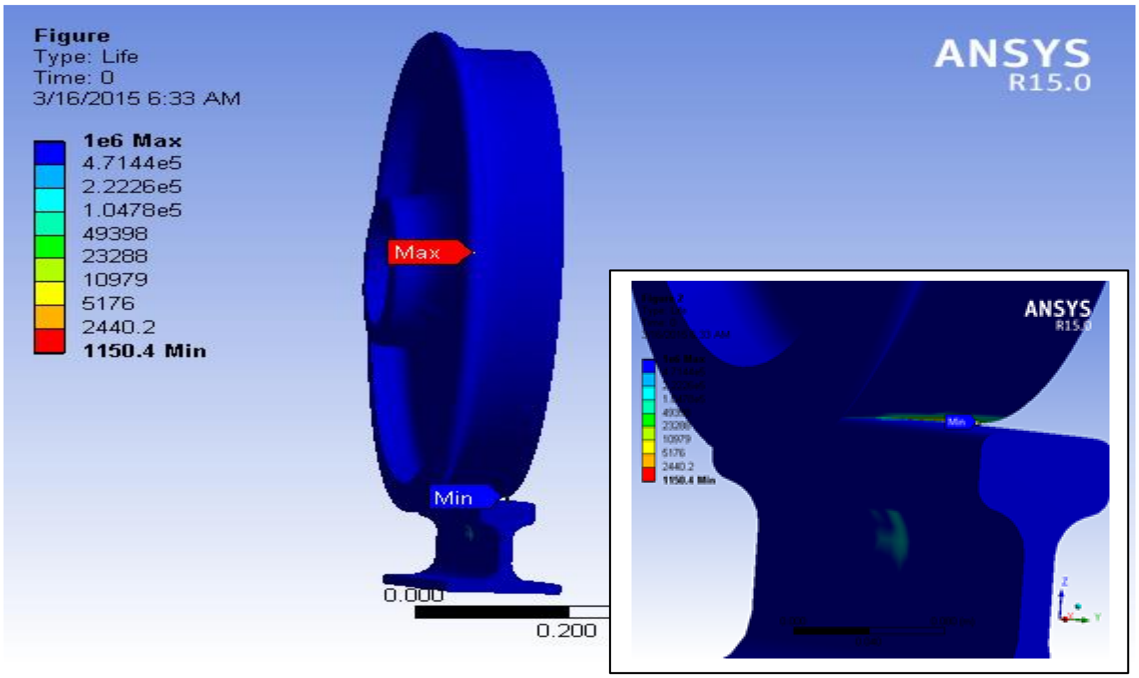

Figure 39: Stress life at contact area for 2.33 m/s slip velocity simulation

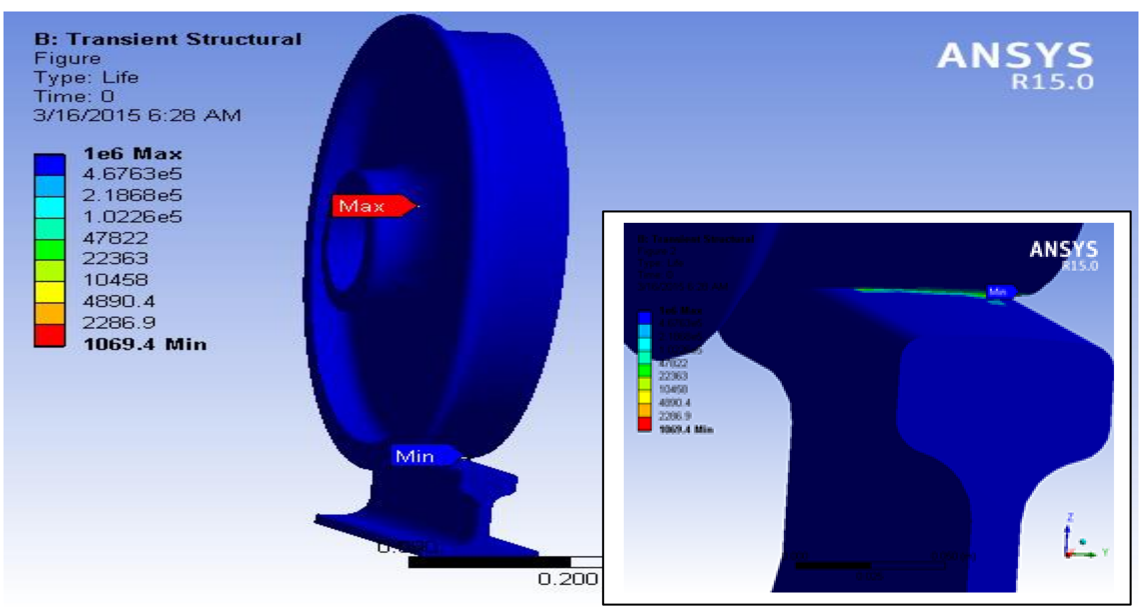

Figure 40: Stress life at contact area for 4.55 m/s slip velocity simulation

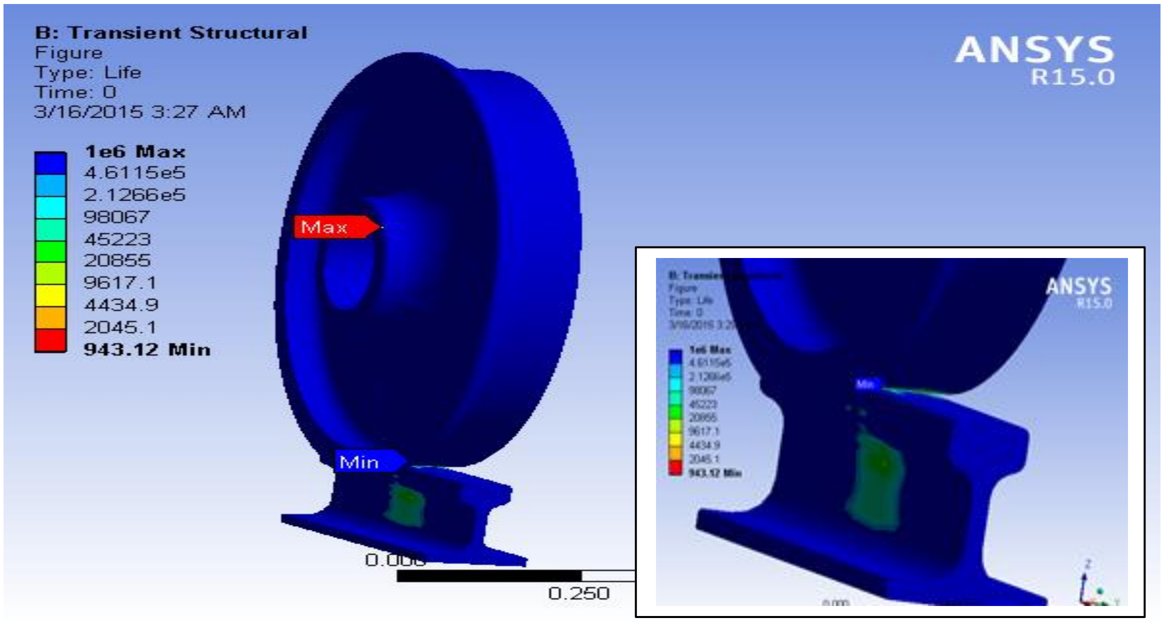

Figure 41: Stress life at contact area for 6.77 m/s slip velocity simulation

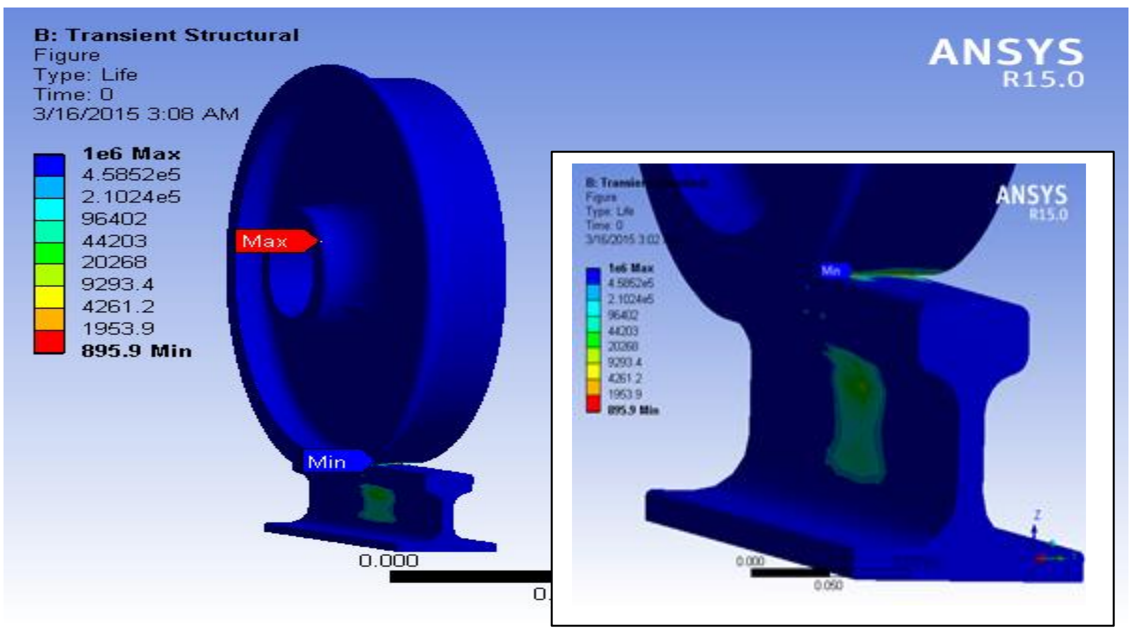

Figure 42: Stress life at contact area for 8.99 m/s slip velocity simulation

The maximum stress life of is 10^6 cycles with alternating stress of 86Mpa. But during combined load analysis the maximum alternating stress is above 600 MPa therefore and stress life cycle is very few. This can be indication of existence of low cyclic fatigue on contact area.

6.2 Discussion

As the loads due to slippage at contact area increase the effect that impose on contact are also increase as we can notice from pictorial graphs presented above. Few micro second slippages create large amount of stress and strain. For the four case of analysis the results are presented the following tables for comparison.

Table 5: Comparison of maximum equivalent thermal stress and combined stress at different slip velocity

Slip velocity (m/s)	Thermal stress (Pa)	Combined stress (Pa)
2.33	$2.783*10^8$	$6.22*10^8$
4.55	$2.850*10^8$	$6.295*10^8$
6.77	$3.697*10^8$	$6.493*10^8$
8.99	$5.013*10^8$	$6.600*10^8$

The equivalent stress in combined load is the sum of the stress created mechanical and thermal load so its value is high form individual stress. Almost for the four case of simulation equivalent stress is higher than yield strength of the material.

Table 6: Comparison of maximum thermal strains at different slip velocity

Slip velocity (m/s)	2.33	4.55	6.77	8.99
Max. thermal strain (m/m)	0.0003117	0.0007558	00.01274	0.001412

Thermal strain created in the contact by presence of contact frictional heating. As can be notice form comparison table for minimum slip velocity analysis and simulation the thermal strain at contact will be less and the stress life on contact area material is be longer.

Table 7: The of value of maximum elastic and plastic strain from combined loads

Slip velocity (m/s)	Max. elastic strain (m/m)	Max. plastic strain (m/m)
2.33	0.003175	0.000710
4.55	0.003389	0.000739
6.77	0.003691	0.000798
8.99	0.003856	0.000972

Solid187 element type was used to model wheel and rail in the workbench. The element is capable of giving plastic stress output for the loads beyond elastic limit. The normal and tangential stresses together with high thermally stresses may lead to higher levels of plastic deformation when compared to case with only the mechanical loads. A wheel sliding on a rail may cause severe thermal damage on the rail surface. The working hardening properties exhibits the plasticity and nonlinear response of the material.

Table 8: Comparison of minimum stress life during combined loads condition

Slip velocity (m/s)	2.33	4.55	6.77	8.99
Min. stress life (cycle)	$1.15*10^3$	$1.06.4*10^3$	943.12	895.9

The stress life is very small for high value slippage which can results low cyclic fatigue. Stress life due to mechanical load is 10 higher than stress life during 2.33m/s slippage. For increased value of slippage 100 times lower stress life will be notice. This is because of existence of thermal load on contact area.

CHAPTER SEVEN

CONCLUSION AND RECOMMENDATION

7.1 Conclusion

The effects of thermo-mechanical load for carbon steel rail-wheel at contact area indirectly analyzed using semi analytical FE analysis statically. The analysis and simulation is carried out at constant coefficient of friction vehicle that have 33.4 m/s velocity and slips at 2.33, 4.55, 6.77and 8.99 m/ s respectively. The simulation is focus on contact area for average time 0.16 micro second a time require to cross contact area. Beside temperature dependent material is included for the simulation. The distribution of the heat flux along contact area is assumed to be constant. With Kinematic hardening property the plastic strain amount is increase as slip velocity increase and stress life is short when compared to less slip load contact condition. Thermal stress and strain induced due to friction heat during slippage crate challenge on the strength of the rail and wheel material. I can summarize the results of the investigations in the current study as follows;

- The value of maximum equivalent von mises stress higher in combined load than the values during mechanical load only. Beside, maximum equivalent von mises stress increase with increase value of slip velocity.
- Stress life of wheel and rail material at contact area is highly affected by existence of slippage on dry rail-wheel contact condition for constant friction coefficient.
- Based on analytical analysis results, temperature increase to extreme values when slip velocity increase indefinitely.
- The values of maximum temperature and combined equivalent von mises stress notice in this simulation are 400 ^{o}C and 660 M pa which are occur 8.99 m/s slip velocity loads simulation.
- Slippage creates heating of rail-wheel contact area together with mechanical load the fatigue life the material highly reduces.

- The amount plastic strain increased by frictional heating for high value of slippage simulation of. When we compared to without surface temperature analysis only elastic strain area notice on contact area.

7.3 Recommendations

An accurate thermal–mechanical analysis of rail wheel contact is critical to understand effect on rail–wheel material. The main cause of thermal and mechanical load at contact area is wheel slippage or sliding .Slippage is a well know problem in rail way industries and should need to be control in order to minimize thermal loads and low cyclic fatigue of rail-wheel material.

High amount of heat can be generating from contact slippage special if axle lock happed during train startup time or decelerating near stations. Cooling mechanism is required in order to reduce contact temperature. Surface temperature above the melting point of the material is predicated through theoretical analysis. If this let to happen, the rail surface will burn and cause rail brakeage specially for full slippage situation

One of the methods of controlling slippage is through adhesion.by introducing friction modifier like sand minimizing the slippage is possible. Beside, timely clearing rails from dirty material and contaminate is helpful in controlling slippage.

Now days, most locomotive are equipped with automatic anti-slip controllers. The efficiency and effectiveness of Ethiopian railway cars anti slip controller's facility should be tested timely .The severity of the effect of slippage high in the time for braking than during traction. The driver should be alert for controlling wheel slippage especially during applying brake.

Preventive maintenance through timely re-profiling of rail and wheel is important order to reduce slippery surfaces. Specific service distance for re-profiling should be allowed. Finally Better strength material that can resist thermal and mechanical load is needed to be considered for longer life and safe operation of railway system.

7.4 Future works

During the analysis the effect of slippage effect on rail-wheel material, there are a lot of problems to be solved. However, because of the broad applications of contact mechanics, in this paper the analysis is limited to the stress and strain analysis of contact area during slippage under thermal and mechanical loads statically. The progress made so far in identifying the place of failure, failure causes and considering different types of track play a great role on the future works of minimizing contact slippage problems.

Finally, some suggestions are listed below for future work as extension and continuity of this paper.

- Hysteresis analysis of contact surface due to combine thermal and mechanical load.
- FE analysis of low cyclic fatigue and profile change and wear of rail-wheel materials during slippage by using the full licensed software.
- Full experimental testing and analysis of monotonic and cyclic strength properties of the rail and wheel used in Ethiopian railway.
- Wear analysis and simulation of contact area during slippage considering thermal and mechanical loads.
- The study of slippage effect on rail- wheel materials by experimental testing the material property with detail FEM shakedown for various slippage conditions.
- Slippage controlling mechanism by means of rail-wheel contact adhesion modifiers.
- Slippage controlling mechanism by automatic slip control methods etc...are the things that need to be addressed.

References

[1] M. A. TANVIR,,Temperature rise due to slip between wheel and rail -an analytical solution for hertzian contact, Wear 61, 1980,P 295-308.

[2] Lei Wu, Zefeng Wen, Wei Li, Xuesong Jin,Thermo-elastic–plastic finite element analysis of wheel/rail sliding contact, Wear 271 ,2011, P437–443

[3] H.Demimonde, S. Beretta, A. Kapoor, Rail life prediction for tramcars under full slip regime, School of Mechanical and Systems Engineering, Newcastle University, Newcastle upon Tyne, NE1 7RU, UK.

[3] Pramod Murali Mohan,Analysis of Railway Wheel to study Thermal and Structural Behavior, International Journal of Scientific & Engineering Research, Volume 3, Issue 11, November-2012

[4] Petr Pichlík, Jiří Zděnek,Overview of Slip Control Methods Used in Locomotives, Transactions on Electrical Engineering, Vol. 3 ,2014, No. 2

[5] Azade Haidari & Parisa Hosseini-Tehrani ,Fatigue Analysis of Railway Wheels Under Combined Thermal and Mechanical Loads, Center of Excellence in Railway Transportation, School of Railway Engineering, Iran, 25 Nov 2013

[6] Railway applications: Wheel sets and Bogies - Wheels - Product requirements, EN 13262:2004+A2

[7] Railway applications: Track - Rail - Part 1: Vignole railway rails 46 kg/m and above required by, EN 13674-1:2011

[8] ANSYS 15, Rate independent plasticity theory reference

[9] Jay Prakash Srivastava, P.K. Sarkar1 and Vinayak Ranjan ,An Approximate Analysis for Hertzian Elliptical Wheel-Rail Contact Problem ,Indian School of Mines, 1955, Dhanbad,India

[10] Jean-Bernard Ayasse and Hugues Chollet, Handbook of rail vehicle dynamics, Taylor and Francis Group, 2006

[11] Martin Ertz, Klaus Knothe, Comparison of analytical and numerical methods for the calculation of temperatures in wheel/rail contact,Wear 253, 2002, P498–508

[12] R. Lunden, Contact region fatigue of railway wheels under combined mechanical rolling pressure and thermal brake loading, Wear 144, 1991, P57–70

[13] F.D.Fischer, E.Werner, W.-Y.Yan,Thermal stress for fractional contact in rail wheel system, ELSEVIER SCIENCE S.A, Wear 211, 1997, P156-163.

[14] George TUMANISHVILI*,Merab CHELIDZE, Victor ZVIADAURI ,Loading and damageability of wheels and rails; Transport Problems journal, Volume 4 Issue 4, 2009

[15] Briony Crofta, Chris Jonesb and David Thompson, Velocity-dependent friction in a model of wheel–rail rolling contact and wear, Vehicle System Dynamics Vol. 49, No. 11, November 2011, P1791–1802

\

Annex: Important tables

Table 9: Hertz coefficient m and n quantities [10]

θ(deg)	m	n	θ(deg)	m	n	θ(deg)	m	n
0.5	61.4	0.1018	10	6.604	0.3112	60	1.486	0.717
1	36.89	0.1314	20	3.813	0.4125	65	1.378	0.759
1.5	27.48	0.1522	30	2.731	0.493	70	1.284	0.802
2	22.26	0.1691	35	2.397	0.530	75	1.202	0.846
3	16.5	0.1964	40	2.136	0.567	80	1.128	0.893
4	13.31	0.2188	45	1.926	0.604	85	1.061	0.944
6	9.79	0.2552	50	1.754	0.641	90	1.0	1.0
8	7.86	0.285	55	1.611	0.678			

Source: Railroad vehicle dynamics: A computational approach (2008)

Table 10: Kalker coefficient table from reference [10]

	g	C_{11}			C_{22}			$C_{23} = -C_{32}$			C_{33}		
		$\sigma = 0$	1/4	1/2	$\sigma = 0$	1/4	1/2	$\sigma = 0$	1/4	1/2	$\sigma = 0$	1/4	1/2
	0.0	$\pi^2/4(1-\sigma)$			$\pi^2/4 = 2{,}47$			$\pi\sqrt{g}/3$	—	—	$\pi^2/16(1-\sigma)g$		
a/b	0.1	2.51	3.31	4.85	2.51	2.52	2.53	0.334	0.473	0.731	6.42	8.28	11.7
	0.2	2.59	3.37	4.81	2.59	2.63	2.66	0.483	0.603	0.809	3.46	4.27	5.66
	0.3	2.68	3.44	4.80	2.68	2.75	2.81	0.607	0.715	0.889	2.49	2.96	3.72
	0.4	2.78	3.53	4.82	2.78	2.88	2.98	0.720	0.823	0.977	2.02	2.32	2.77
	0.5	2.88	3.62	4.83	2.88	3.01	3.14	0.827	0.929	1.07	1.74	1.93	2.22
	0.6	2.98	3.72	4.91	2.98	3.14	3.31	0.930	1.03	1.18	1.56	1.68	1.86
	0.7	3.09	3.81	4.97	3.09	3.28	3.48	1.03	1.14	1.29	1.43	1.50	1.60
	0.8	3.19	3.91	5.05	3.19	3.41	3.65	1.13	1.25	1.40	1.34	1.37	1.42
	0.9	3.29	4.01	5.12	3.29	3.54	3.82	1.23	1.36	1.51	1.27	1.27	1.27
b/a	1.0	3.40	4.12	5.20	3.40	3.67	3.98	1.33	1.47	1.63	1.21	1.19	1.16
	0.9	3.51	4.22	5.30	3.51	3.81	4.16	1.44	1.59	1.77	1.16	1.11	1.06
	0.8	3.65	4.36	5.42	3.65	3.99	4.39	1.58	1.75	1.94	1.10	1.04	0.954
	0.7	3.82	4.54	5.58	3.82	4.21	4.67	1.76	1.95	2.18	1.05	0.965	0.852
	0.6	4.06	4.78	5.80	4.06	4.50	5.04	2.01	2.23	2.50	1.01	0.892	0.751
	0.5	4.37	5.10	6.11	4.37	4.90	5.56	2.35	2.62	2.96	0.958	0.819	0.650
	0.4	4.84	5.57	5.57	4.84	5.48	6.31	2.88	3.24	3.70	0.912	0.747	0.549
	0.3	5.57	6.34	7.34	5.57	6.40	7.51	3.79	4.32	5.01	0.868	0.674	0.446
	0.2	6.96	7.78	8.82	6.96	8.14	9.79	5.72	6.63	7.89	0.828	0.601	0.341
	0.1	10.7	11.7	12.9	10.7	12.8	16.0	12.2	14.6	18.0	0.795	0.526	0.228

Table 11: Adding of thermal (A) mechanical (B) material property data for combined load at 100 ^oC surface temperature analyses.

A

Outline of Schematic A2: Engineering Data

	A	B	C	D
1	Contents of Engineering Data		ource	Description
2	Material			
4	Carbon steel			Fatigue Data at zero mean stress comes from 1998 ASME BPV Code, Section 8, Div 2, Table 5-110.1

Table of Properties Row 2: Density

	A
1	Temperature (C)
2	100
*	

Properties of Outline Row 4: Carbon steel

	A	B	C	D	E
1	Property	Value	Unit		
2	Density	7818	kg m^-3		
3	Isotropic Thermal Conductivity	47.1	W m^-1 C^-1		
4	Specific Heat	487.5	J kg^-1 C^-1		

B

chematic B2: Engineering Data

	A	B	C	D
1	Contents of Engineering Data		ource	Description
2	Material			
4	Carbon steel			Fatigue Data at zero mean stress comes from 1998 ASME BPV Code, Section 8, Div 2, Table 5-110.1

Properties of Outline Row 4: Carbon steel

	A	B	C	D	E
1	Property	Value	Unit		
3	Isotropic Secant Coefficient of Thermal Expansion				
4	Coefficient of Thermal Expansion	1.22E-05	C^-1		
5	Reference Temperature	20	C		
6	Isotropic Elasticity				
7	Derive from	Young's Modulus and Poisso...			
8	Young's Modulus	2.03E+11	Pa		
9	Poisson's Ratio	0.286			
10	Bulk Modulus	1.581E+11	Pa		
11	Shear Modulus	7.8927E+10	Pa		
12	Bilinear Kinematic Hardening				
13	Yield Strength	5.6E+08	Pa		
14	Tangent Modulus	1.5E+10	Pa		
15	Alternating Stress Mean Stress	Tabular			
16	Interpolation	Semi-Log			
17	Scale	1			
18	Offset	0	Pa		
19	Tensile Yield Strength	6E+08	Pa		
20	Compressive Yield Strength	6E+08	Pa		
21	Tensile Ultimate Strength	9E+08	Pa		

ADDIS ABABA UNIVERSITY

ADDIS ABABA INSTITUTE OF TECHNOLOGY

SCHOOL OF MECHANICAL AND INDUSTRIAL ENGINEERING

DECLARATION

I, the undersigned, declare that this thesis is my original work and has not been presented for any degree in any university and all the sources of materials used for the thesis have been duly acknowledged.

Abdulhakim Merdassa	__________________	__________________
Name	Signature	Date